Automatic Analysis of Neuro-biological Signals Based on Expert Knowledge

BY

ZHANFENG JI

A dissertation submitted in partial fulfillment of
the requirements for the Doctor of Philosophy degree
in Advanced Systems Control Engineering,
Graduate School of Science and Engineering,
Saga University

September, 2011

Supervisor: PROFESSOR SATORU GOTO

Abstract

Nowadays, automatic analysis of neuro-biological signals plays more and more important roles in both clinical diagnosis and laboratory research. However, neuro-biological signals are inevitably contaminated by various artifacts. The analysis without considering the artifacts would lead to mis-interpretation results. Therefore, an available signal selection technique is necessary to be developed for obtaining accurate and reliable results. In this paper, a model of real-time data classification system for accurate analysis of neuro-biological signals was proposed. The proposed model can be utilized for various research purposes. As an example, a physical system to analyze the relationship between characteristics of electroencephalogram (EEG) and electrocardiogram (ECG) was developed. The results indicated that the real-time system was effective for available signals selection. With the developed real-time system, the quality of signals can be monitored during the recording process.

Epilepsy is one of the most common neurological diseases. Automatic EEG spike detection provides valuable information for epilepsy diagnosis. In the past 30 years, a number of algorithms were proposed. However, the basic idea of most algorithms is to identify spike activities. Most automatic spike detection systems in the scalp EEG focused on the characteristics of “spike”. However, the characteristics of “false positives” (FPs) have not been fully studied. In this paper, we proposed a system contains a series of algorithms to eliminate FPs and a template method to confirm spikes. The system used large area context available on 49 channels from two common montages. The impact of slow-waves after spikes was taken into consideration, as well as the information from single channel, multi-channel, and whole recording. Two types of FPs were identified in this paper. The ones from typical artifacts were identified by analysis of background EEG activities, and the ones from other EEG activities were declared by spatial and temporal characteristics of spike activities. Finally, a multi-channel template method was used to assess the performance of proposed system. The system was evaluated using 17 routine EEG recordings. Spike activities were observed in 6 of them. Effective multi-channel templates were extracted from 4 recordings containing frequent spikes. The least selectivity was 92.6% and the most false positive rate was 0.26 per minute. Proposed algorithms for elimination of FPs are also suitable for other algorithms to enhance performance since most FPs can be identified while few true spikes are eliminated.

In practice application, real-time spike detection system is more useful. The algorithm based on identifying non-spike activities for off-line analysis was improved for real-time application using real-time template. Template method is a typical spike detection method. It was not widely employed because of the difficulty of making template. Our results suggested that multi-channel template is meaningful and effective for real-time detection. Spike activities can be detected with a delay of about 2 s. We also designed a simple user-friendly monitor interface for monitor and review spike events in real-time.

Approval

Graduate School of Science and Engineering
Saga University
Honjomachi, Saga 840-8502, Japan

CERTIFICATE OF APPROVAL

Ph.D DISSERTATION

This is to certify that the Ph.D Dissertation of
ZHANFENG JI

has been approved by the Examining Committee
for the dissertation requirement for the Doctor of
Philosophy degree in Advanced Systems Control Engineering
at the September, 2011 graduation.

Dissertation committee:

Supervisor, PROF. SATORU GOTO
Dept. of Advanced Systems Control Engineering

Member, PROF. EIJI TAKAHASHI
Dept. of Advanced Systems Control Engineering

Member, PROF. KAZUHIRO MURAMATSU
Dept. of Advanced Systems Control Engineering

Member, ASSOC. PROF. TAKENAO SUGI
Dept. of Advanced Systems Control Engineering

Copyright ©

Dedication

To my dear parents and to my lovely son and wife
they contribute me great encouragement and support
in all my endeavors for success.

and

To all my loving teachers, who taught and
equipped me with discipline and knowledge.

Acknowledgments

The author expresses heartfelt gratitude to his supervisor, Professor Satoru Goto for the valuable guidance and encouragement. It has so indispensable through the recent three years of her academic and research career in Saga University, Japan. The author extends special thanks to Professor Masatoshi Nakamura for his valuable guidance and suggestions. The author also extends sincere gratitude to his co-supervisor, Associate Professor Takenao Sugi for effective comments and kindly guidance.

The author extends his sincere gratitude to Professor Eiji Takahashi, and Professor Kazuhiro Muramatsu for their corporation while being his supervisors.

The author extends his gratitude to Doctor Akio Ikeda of the Kyoto University School of Medicine, Professor Takashi Nagamine of the Sapporo Medical University and Professor Hiroshi Shibasaki of the Takeda General Hospital for their valuable comment from clinical view point.

The author extends sincere thanks to Prof. Xingyu Wang, Department of Automation, East China University of Science and Technology, for his support and help.

Contents

List of Figures

List of Tables

Chapter 1

Introduction

1.1 Nervous system, brain, and neuro-biological signals

The nervous system is an organ system containing a network of specialized cells called neurons that coordinate the actions of an animal and transmit signals between different parts of its body. In humans the nervous system consists of two parts, central and peripheral. The central nervous system of humans contains the brain, spinal cord, and retina. The peripheral nervous system consists of sensory neurons, clusters of neurons called ganglia, and nerves connecting them to each other and to the central nervous system. These regions are all interconnected by means of complex neural pathways. The autonomic nervous system (ANS) is the part of the peripheral nervous system that acts as a control system functioning largely below the level of consciousness, and controls visceral functions. The ANS affects heart rate, digestion, respiration rate, salivation, perspiration, diameter of the pupils, and urination. Most of its actions are involuntary, such as breathing, work in tandem with the conscious mind.

For central nervous system, the brain is the moat important organ for human beings. It is the center of the central nervous system. The brain is extremely complex. It controls the other organ systems of the body, either by activating muscles or by causing secretion of chemicals such as hormones. The brain monitors and regulates the body's actions and reactions. It continuously receives sensory information, and rapidly analyzes this data and then responds accordingly by controlling bodily actions and functions. The cerebral cortex of the brain is nearly symmetrical, with left and right hemispheres. Each hemisphere is conventionally divided into four lobes, including frontal lobe, parietal lobe, occipital lobe, and temporal lobe.

Despite rapid scientific progress, much about how nervous system and brain work remains a mystery. In order to investigate nervous system and brain, many research fields related to neuro-biological signals have been developed. Neuro-biological

signals contain electroencephalogram (EEG), electrocardiogram (ECG), electrooculogram (EOG), and electromyogram (EMG). They have close relationship with human mental/physical functions. EEG is the reflection of brain activities. ECG reflects the muscle movement of heart and the variability of autonomic nervous system. EOG comes from the movement of eyeball. EMG records the muscle activities at a certain part of the body. EEG and ECG are more important in clinical diagnosis, and EEG is most complex.

Electroencephalogram is from a German word "Elektroenkephalogramm", named by a German psychiatrist - Hans Berger. EEG is the recording of electrical activity along the scalp produced by the firing of neurons within the brain. Berger was the first person to prove the existence of electric potentials in the human brain using an amplifying machine. Berger recorded the first human EEG in 1924, from his fifteen-years-old son, Klaus. The first frequency he encountered was the 10-hertz range, which at first was called the Berger rhythm, currently called Alpha rhythm brain wave. In 1929, he published the first report on human EEG. In that report, he described and defined the alpha and beta waves. He recorded EEG not only in normal subjects but also in the brain-injured, thereby laying the foundation for the application of the technique to clinical technology. After that, EEG was under intensive study. The alpha waves were especially well developed in recordings over the occipital cortex, and they reduced considerably in amplitude when the eyes were opened.

ECG is the synonym of EKG. In order to avoid confusion with EEG, sometimes medical doctors use EKG, which is from the German word Elektrokardiogramm. ECG is an interpretation of the electrical activity of the heart over time captured and externally recorded by skin electrodes. It is the best way to measure and diagnose abnormal rhythms of the heart. Einthoven assigned the letters P, Q, R, S and T to the various deflections, and described the electrocardiographic features of a number of cardiovascular disorders. In 1924, he was awarded the Nobel Prize in Medicine for his discovery.

1.2 EEG rhythms and recording

EEG reflects of the electric activities of apical dendrite of neural cells. It is difficult to measure the electric activity of single neural cell. And it is dangerous to record the electric activity of neural cells directly on the cortex of brain. As a result, the EEG signals recorded on the scalp are very weak, as shown in Fig. 1.1.

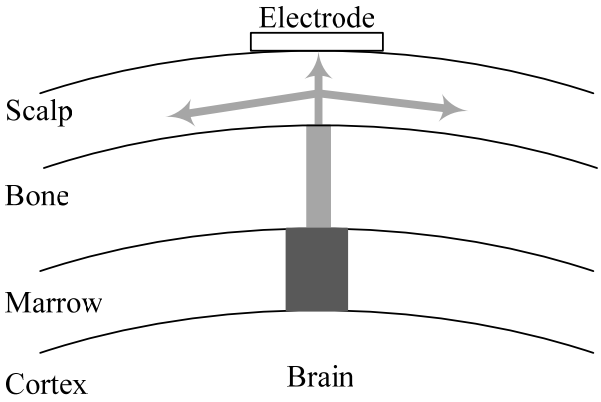

Fig. 1.1 The EEG signals from brain to electrode

Even though the electrical power is very limited, it does occur in very specific ways that are characteristic of the human brain. Electrical activity emanating from the brain is displayed in the form of EEG. There are several categories of these EEG waves, ranging from the most activity to the least activity.

From the viewpoint of frequency band, the basic EEG rhythms consist of delta, theta, alpha and beta waves.

Beta: 14-30Hz. Beta waves represent arousal. The beta waves are of relatively low amplitude, and are the fastest of these four different rhythms. When the brain is aroused and actively engaged in mental activities, it generates beta waves. Beta waves are characteristics of a strongly engaged mind, such as a person in active conversation, making a speech.

Alpha: 8-13Hz. Alpha waves represent non-arousal. Alpha waves are slower, and higher in amplitude. Alpha waves can be seen when a person has completed a task and sits down to rest, takes time out to reflect or meditate, or takes a break from a conference and walks in the garden.

Theta: 4-7Hz. Theta waves are typically of even greater amplitude and slower frequency. Theta waves are generated in a person who has taken time off from a task and begins to daydream, or a person who is driving on a freeway and discovers that they can not recall the last five miles.

Delta: 0.5-3Hz. Delta waves are of the greatest amplitude and slowest frequency. They never go down to zero because that would mean that you were brain dead. But, deep dreamless sleep would take you down to the slowest frequency.

When we go to bed and read for a few minutes before attempting sleep, we are likely to be in low beta. When we put the book down, turn off the lights and close our eyes, our brain waves will descend from beta, to alpha, to theta and finally, when we fall asleep, to delta.

EEG signals are very weak, usually less than 200 uV. The electrode placement of international 10-20 system is shown in Fig. 1.2. The scalp is subdivided by intervals of 10% to 20% and to designate the site where an electrode will be placed. A

minimum of 21 electrodes are recommended for clinical study, although digital EEG now has the capability for a greater number [1].

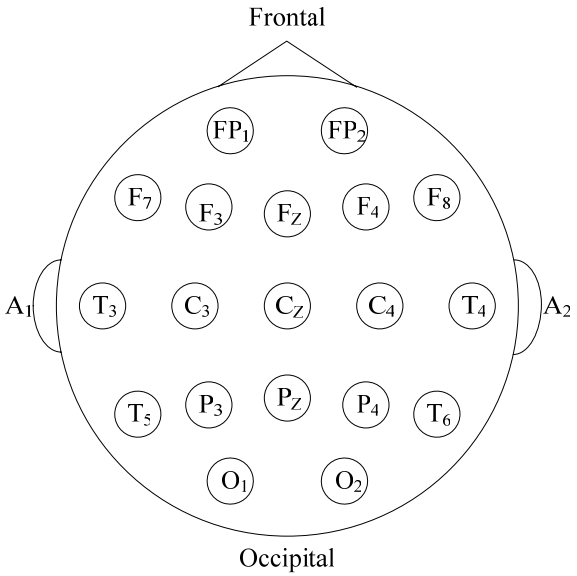

Fig. 1.2 The electrode placement of international 10-20 system (the designation: F_P – frontopolar, F – frontal, T – temporal, O – occipital, P – parietal; the subscription: odd numbers – left, even numbers – right, $_Z$ – midline)

Traditionally, EEG waveforms are recorded on paper. The paper speed used in routine EEG is 30 mm/sec. The amplitude is of 10 uV/mm. In a 1-hour record, more than 10-m EEG papers are generated. These EEG papers can be saved by using digital EEG. The slower paper speed (10 mm/sec) used in sleep EEG is useful as low-frequency activity is better seen at that paper speed. In this case, more papers are needed. Today, digital EEG is recommended as an established substitute for recording, reviewing, and storing EEG signals. It is a clear technical advance over previous paper methods [2].

EEG signals can be recorded with different montages, including referential montage, bipolar montage, and laplacian montage. One advantage of digital recording is that it allows reformatting of the signals with different montages after recording. In referential montage, a common reference electrode is connected to each electrode. In the past, referential recording was also referred to as monopolar recording. The reference electrodes include ipsilateral ear-lobe (A1 and A2); linked ears (A1+A2); and the average reference (the average of all scalp electrodes). In bipolar montage, adjacent electrodes are connected. This montage is popular in clinical diagnosis, especially in visual inspection of spike detection. In laplacian source derivation, voltages at each electrode site are compared with a local average of voltages at immediately surrounding electrodes. For example, for C4, the local average is equal to (F4+P4+CZ+T4)/4.

1.3 ECG and heart rate variability

A typical ECG wave of the cardiac cycle (heartbeat) consists of a P wave, a QRS complex, a T wave, and a U wave, as shown in Fig. 1.3. The QRS complex reflects the rapid depolarization of the right and left ventricles. They have a large muscle mass compared to the atria. Therefore, the QRS complex usually has much larger amplitude than the P-wave and T-wave.

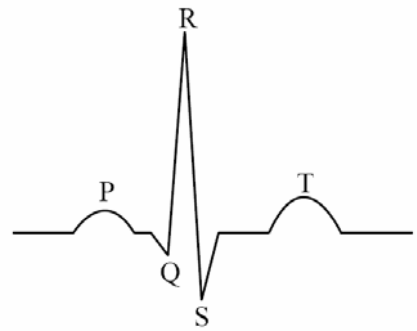

Fig. 1.3 A typical ECG wave

ECG signals are much stronger than EEG signals. The amplitude of the QRS complex is usually more than 1 mV. A 12-lead ECG is commonly used in clinical recording.

Heart rate variability is the most popular research topic in ECG studies. It was first mentioned by Hon and Lee in 1963 [3]. They noted that fetal distress was preceded by alterations in interbeat intervals before any change in the heart rate. Ten years later, Sayers reported the physiological rhythms in the beat-to-beat heart rate signals [4]. In 1981, Akselrod et al. first applied power spectral analysis to heart rate fluctuations for quantitative evaluation of beat-to-beat cardiovascular control [5]. The understanding of autonomic functions by heart rate spectral analysis is reported in 1985 [6]. Since then, heart rate spectral analysis became a powerful noninvasive tool for quantifying autonomic nervous system activity. Later, Malik et al. pointed out that heart rate variability was a strong predictor of mortality after acute myocardial infarction [7]. After that, a number of papers were published related to heart rate variability [8]-[14].

1.4 Data classification of neuro-biological signals

1.4.1 Artifacts

Neuro-biological signals are inevitably disturbed by various factors. Artifacts denote the signals which against the research purpose. Artifacts may originate from a variety of sources. Generally speaking, artifacts are divided into two groups: physiological and non-physiological. Physiological artifacts are usually generated from the sources in the body but not related to the brain. Non-physiological artifacts are generated from the sources out of the body, such as amplifiers, electrodes, environment, and so on.

EEG signals are easily to be contaminated by kinds of artifacts. The artifacts in EEG are related but not limited to eye movement, muscle activity, heart beat, body movement, electrode, amplifier, and power supply. Comparing with EEG, ECG signals are much stronger. Artifacts should be defined according to specific research purposes. The major sources of artifacts are body movement and muscle activity.

1.4.2 Automatic detection technique and problems

Artifacts rejection or removal is crucial for accurate analysis of neuro-biological signals. Contaminated signals lead to misinterpretation results. Many algorithms have been tried for the rejection or removal of artifacts in EEG [15-23]. But few papers considered the artifacts in ECG [12-14].

The relationship between different neuro-biological signals including EEG, ECG, EOG, and EMG is potential to be an interesting research topic in future, especially of real-time application. Few papers concentrated on the relationship between the neuro-biological signals. Moreover, the advanced algorithms are not proper for real-time application.

1.5 Automatic EEG spike detection

1.5.1 Spike activities

Epilepsy is one of the most common neurological diseases, affecting more that 40 million people in the world. EEG test has become an inevitable procedure in diagnosis of epilepsy. In the EEG of epilepsy patients, spikes or sharp waves can be seen clearly. Conventionally, the EEG waves are visual inspected by doctors. But for long-term

EEG recording, visual inspection is time-consuming. It is necessary to introduce computer-assistant technologies. Spike and sharp wave were defined by Chatrian et al. in 1974 [24]. “A spike is a transient, clearly distinguished from background activity, with pointed peak at conventional paper speeds and a duration from 20 to under 70 ms, i.e., 1/50 to 1/14 s, approximately. Main component is generally negative relative to other areas. Amplitude is variable. Sharp wave is with a duration from 70 to under 200 ms.” This definition is incomplete because it lacks features differentiating some other activities such as eye blinks and electrode artifacts. In practice, the following characteristics are helpful for judgment of spike activities:

- Appearing in multi-channels
- Clear focus
- Clear slow-wave

Typical waveforms of spike activities are shown in Fig. 1.4 (a). The distribution of referential montage and bipolar montage channels are shown in Fig. 1.4 (b). In this example, clear spike waveforms are observed in F8 and T4, and the focus is identified between F8 and T4.

Since the diagnosis of epilepsy is complex, EEG test is only an assistant tool. However, the misinterpretation or over interpretation of EEG is serious.

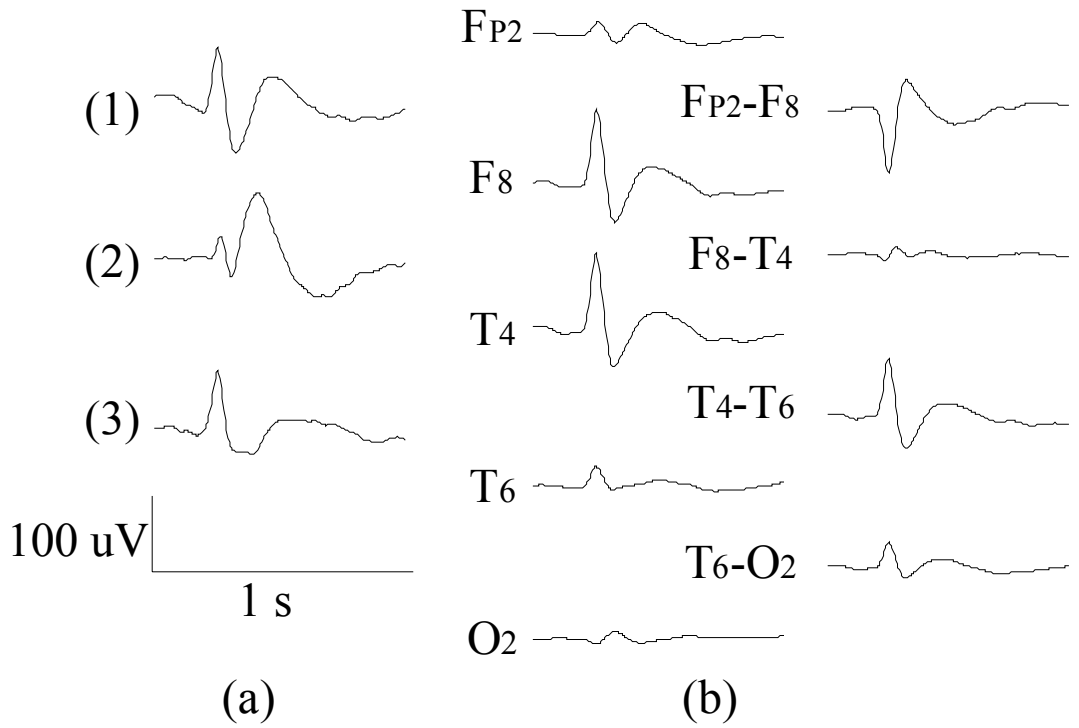

Fig. 1.4 Examples of spike waveform. (a) Typical waveforms: (1) clear spike with clear slow-wave; (2) small spike with clear slow-wave; (3) sharp-wave without slow-wave. (b) The distribution of spike activity.

1.5.2 Development of automatic spike detection

Automatic spike detection technique has been developed for more than 30 years. A number of research groups have tried different methods. Methods for the detection of epileptiform events can be broadly divided into two main categories: temporal detection methods that exploit the EEG's temporal characteristics, and spatial detection methods that base detection on the results of an implicit or explicit source analysis.

As shown on the left of Fig. 1.5, review papers are listed. They reviewed published automatic spike detection methods in the viewpoint of algorithm [25] - [32]. The history was grouped into three periods by Harner: (1) beginnings, 1972-1985; (2) new technologies, 1985-2002, and (3) the present, 2002-2009 [30]. Here, I would like to describe the development of history from the viewpoint of research groups. In the following text, the research group leading by Jean Gotman is abbreviated as G group, James D Frost Jr as F group, Richard D Jones as J group, Scott B Wilson as W group. The other groups are divided into artificial neural network (ANN), wavelet transform (WT), multi-methods algorithm, and other algorithms.

- **Jean Gotman**

Gotman is the pioneer in the field of EEG analysis for epilepsy diagnosis. He and his colleges did a lot of meaningful studies [33-47]. Today, many seizure monitoring systems use the Gotman algorithm or its variation for EEG spike detection.

Spike detection. In 1976, he and Gloor proposed their mimic method, which is still widely used today. In 1979, the method is developed for prolonged EEG recording. In 1991 and 1992, he and Wang improved the method as state-dependent.

Seizure detection. In 1982, he extended his system to automatic seizure detection. The system can perform on-line and simultaneously detect spikes and of seizures. In 1997, G group presented a set of methods for the seizure detection in the newborn, because the features of seizures and EEG background in the newborn are different to those in adults. In 1998, G group integrated their algorithms as one system to assist doctors reviewing prolonged EEG recording. In 2005, G group improved the seizure detection system with onset warning function.

Dipole model. In 1999, G group started to investigate the dipole-modeling method for spike detection. In 2001, G group used independent component analysis with dipole model to separate spikes from background EEG signals. In 2002, G group calculated single dipole source model for each possible spike event. They found that the method performs well for frequent spikes, but not well for rare spikes. In 2003, G group tried to illustrate the variability of the error in dipole modeling of epileptic spikes by using employing a realistic head model. Also in 2003, they used a dipole source algorithm to improve performance of spike detection by identifying false

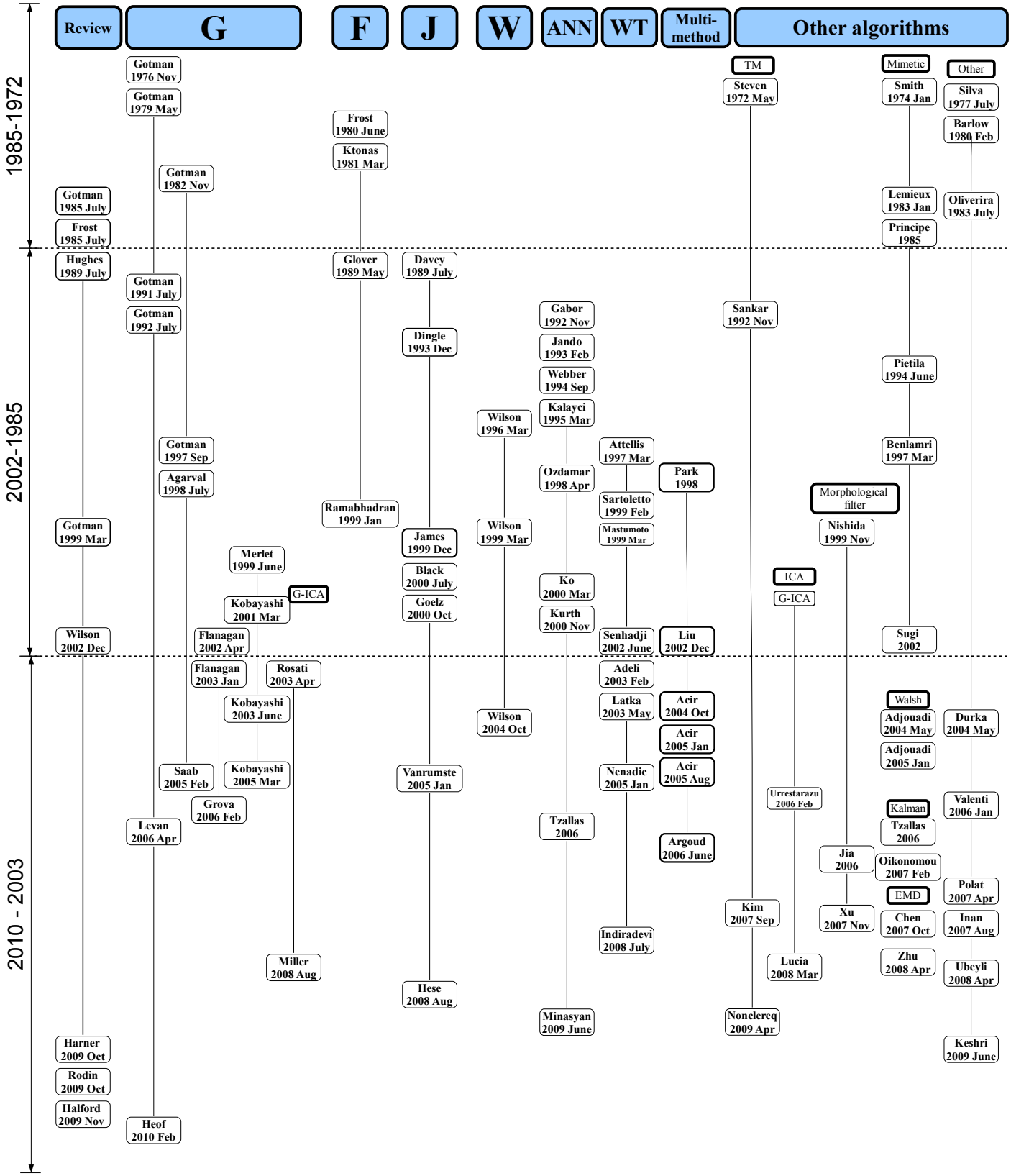

Fig. 1.5 The history of automatic EEG spike detection

detections caused by artifacts. In 2005, their study suggested that, the dipoles clustered at very misleading locations when the source was very large. In 2006, they evaluated the performance of different source localization methods, and suggested that different localization methods should be considered when analyzing real interictal spikes.

In 2010, Hoef et al. evaluated the Gotman system [48]. The Results suggested that the sensitivity is relatively low. When using a lower amplitude threshold and not using advanced artifact rejection, the sensitivity is higher. But the false-positive rate increases with improved sensitivity.

- **James D. Frost**

Frost et al. developed an automatic EEG interpretation system in 1980 [49]. In his review paper of 1985, he emphasized the problems associated with artifact rejection and the need for establishing context-based decision-making processes. Ktonas et al. independently made a quantification of the characteristics of well-defined spikes and sharp waves [50]. The morphological differences between spikes were explained. In 1989, F group proposed their spike detection system [51]. It was a knowledge-based system for the elimination of false positives. The system employed the spatial and temporal context information available on 16 channels of EEG, ECG, EMG, and EOG. This is the only paper considering ECG, EMG and EOG for spike detection. F group improved their system in 1999 [52]. The system emphasized epileptic focus localization.

- **Richard D. Jones**

Jones et al. investigated different methods for spike detection. In 1989, J Group proposed an expert system to detect spike activities [53]. In 1993, they improved the system [54]. Previous expert system is used to detect focal and nonfocal multichannel epileptiform events. Considerable spatial and temporal contextual information are used for detection of epileptiform events and rejection of artifacts. In 1999, the system was further developed. It consisted of three major stages: mimetic, self-organising feature map, and fuzzy logic [55].

In 2000, they investigated the performance of their system for real-time detection during routine clinical recordings [56]. Also in 2000, J Group attempted to use continuous wavelet transform to detect spike activities [57]. In 2005, they investigated the presence and characteristics of apparent non-epileptiform activity arising in the same brain area as epileptiform activity in the EEG of paediatric patients with focal epilepsy. This is the first study to investigate the non-epileptiform activity in the EEG of patients with focal epilepsy [58]. Their latest study was reported in 2008. They presented a spatial detection method, which was improved by including temporal information. Dipole medel was used [59].

- **Scott B. Wilson**

Wilson et al. proposed a multiple monotonic neural network method to detect spike activities in 1999 [60]-[61]. Before that, they had established their EEG data set and investigated the correlation between the visual inspection results of human experts. In 2002, Wilson reviewed the papers from 1976 to 2000 in detail [29]. Then they reported their seizure detection method in 2004 [62].

- **Others**
  - **ANN groups**

Feed forward networks trained by the back propagation algorithm are preferred by most authors. Other networks were also investigated by some authors.

Gabor and Seyal first used ANN for automatic spike detection in 1992 [63]. After them, a number of related studies were reported. In 1993, Jandó et al. investigated back-propagation networks in automatic recognition of EEG spike-and-wave spindle patterns in the rats [64]. In 1994, Webber et al. trained their ANN system by both parameterized and raw EEG data. They suggested that ANN can produce sensitivity and selectivity similar to those of EEGers [65]. In 1995, Kalayci and Ozdamar tried to decrease the input size to the ANN detector by using a wavelet transforms (WT) as a preprocessor [66]. However, in 1998, Ozdamar and Kalayci employed a feed forward ANN using raw EEG signals [67]. In 1999, Wilson et al. employed multiple monotonic neural networks in their perception-based system [61], and Jones Group employed self-organising feature map in their multi-stage system [55]. In 2000, Ko and Chung concluded that spike detection using raw EEG data as input is unlikely to be feasible under the computer technology in 2000 [68]. In the same year, Kurth et al. examined the performance of a pattern-based automated spike detection system with a Kohonen feature map [69]. In 2006, Tzallas et al. proposed a system using different ANN architectures for spikes, EMG, blinks, and sharp alpha waves [70].

  - **WT groups**

As mentioned above, WT method was used by Kalayci and Ozdamar in 1995 for spike detection [66]. In 1997, D'Attellis employed an algorithm based on polynomial spline wavelet transform [71]. In 1999, Sartoretto and Ermani tried single level wavelet analysis for spike detection [72]. Jones Group also tried to use WT in their system [57]. In 2002, Senhadji and Wendling investigated WT together with time-frequency methods [73]. Both are non-stationary signal transforms. In 2003, Latka et al. demonstrated wavelet transform is a relatively simple detection algorithm [74], as well as Adeli in 2003 [75], Nenadic and Burdick in 2005 [76]. Multi-level wavelet approach was proposed by Indiradevi et al. in 2008 [77].

  - **Multi-methods systems**

In 1998, Park et al. proposed a multi-channel spike detection system for long term

EEG monitoring of epilepsy. It consisted of WT, ANN and expert system [78]. In 2002, Liu et al. presented a system using nonlinear filter, WT, ANN, and expert system [79]. In 2005, Acir et al. employed support vector method (SVM) and ANN [80]. In 2006, Argoud et al. reported a system including WT, ANN and expert system [81].

- **Other algorithm groups**

Similar to Gotman, some other authors also investigated mimetic method [82]-[87]. Although template method is one the earliest algorithm, it was only used in a few papers [88]-[91]. Other advanced algorithms were also investigated, such as ICA [40] [92] [93], Kalman filter [94] [95], Walsh transform [96] [97], morphological filter [98]-[100], Empirical Mode Decomposition (EMD) [101] [102], inverse digital filter [103], pattern recognition [104], time-frequency method [105], data mining model [106], decision tree classifier [107], fuzzy C-means clustering [108], mixture of experts network [109], deterministic finite automata [110], and focus method [111].

1.5.3 Difficulties

Over the past 30 years, kinds of algorithms were investigated. But none of them are widely accepted because of false positive detections. Misinterpretation or over-interpretation of EEG recording is a serious problem [112]-[116].

Almost all the researchers attempted to answer “what is a true spike event”. In fact, we can not identify an event as a true spike event with 100 percent confident by the characteristics used in published papers. On the contrary, we can identify an event as a non-spike event with countless reasons.

From the viewpoint of human, before identifying a true spike event, countless non-spike events have been rejected. Only if an event does not belong to any non-spike activities, it is possible to be spikes. In other words, the results of true spike events by visual inspection can be viewed as the results after identifying all non-spike events. Therefore, to answer “what is a non-spike event” is more crucial. However, it is difficult to list all the situations of non-spike events.

1.6 Aim of the thesis

Almost all automatic analysis systems for neuro-biological signals consist of four stages: (1) data acquisition; (2) pre-processing; (3) main processing and (4) results and information. The aims of this research work are in twofold. First, in order to obtain reliable results, it is necessary to recognize whether the signals are available or unavailable in pre-processing stage. In case of long-term recordings, unavailable signals should be removed before any feature analysis. Therefore, we endeavor to

develop a real-time data classification model. Second is related to main processing stage. We attempt to explore a new automatic EEG spike detection algorithm for epilepsy diagnosis. Most research groups concentrated on the characteristic of spike activities. It is interesting to investigate a spike detection algorithm based on elimination of non-spike activities. Besides, we also make effort on real-time application.

1.7 Thesis structure

The structure of the thesis is shown in Fig. 1.6. **Chapter 1** introduces the background knowledge of neuro-biological signals and automatic detection techniques.

Chapter 2 focuses on a real-time data classification model based on artifacts detection. The proposed model can be utilized for various research purposes. As an example, a physical system to analyze the relationship between characteristics of EEG and ECG was established.

Chapter 3 proposes an off-line spike detection system. The system contains a series of algorithms to eliminate false positives (FPs) and a template method to confirm spikes. The system used large area context available on 49 channels from two common montages. The impact of slow-waves after spikes was taken into consideration, as well as the information from single channel, multichannel, and whole recording. Two types of FPs were identified in this chapter. The ones from typical artifacts were identified by analysis of background EEG activities, and the ones from other EEG activities were declared by spatial and temporal characteristics of spike activities. Finally, a multi-channel template method was used to assess the performance of the proposed system.

In **Chapter 4**, a real-time spike detection system was developed based on real-time multi-channel template method. The system is effective for the patients with frequent spike activities. However, it should be noted that automatic detection is an assistant tool, since the results must be identified by EEGers before clinical judgment.

In **Chapter 5**, the conclusions about real-time data classification and real-time spike detection algorithm are discussed. Related future work is also described.

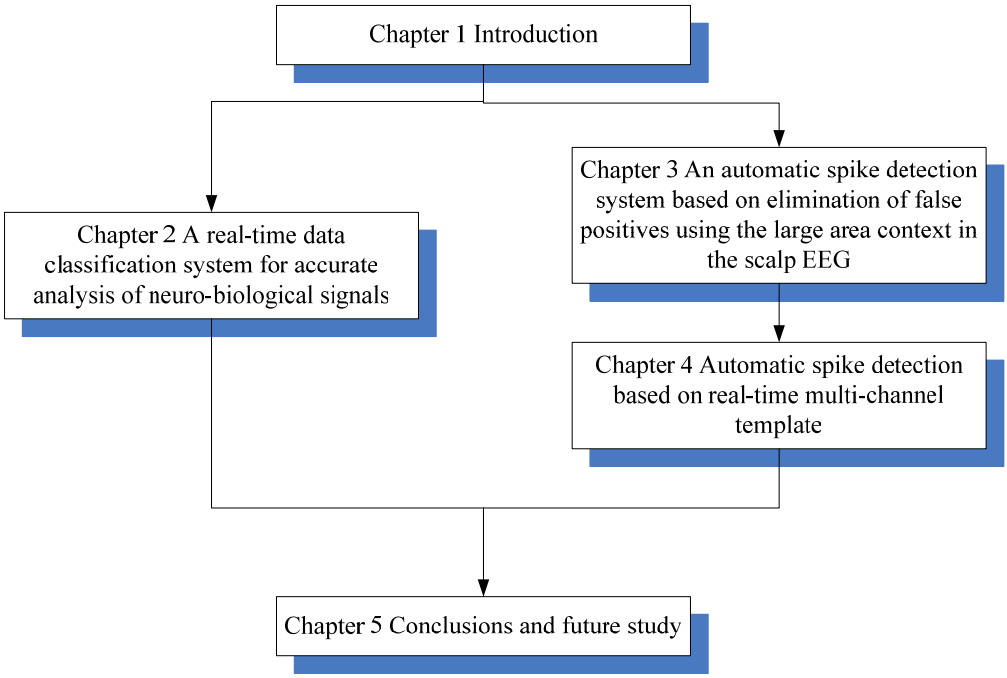

Fig. 1.6 Thesis structure

Chapter 2

A real-time data classification system for accurate analysis of neuro-biological signals

2.1 Introduction

The neuro-biological signals containing electroencephalogram (EEG), electrocardiogram (ECG), electrooculogram (EOG) and electromyogram (EMG) have close relationship with human mental/physical functions. EEG is the reflection of brain activities. ECG reflects the muscle movement of heart and the variability of autonomic nervous system. EOG comes from the movement of eyeball. EMG records the muscle activities at a certain part of the body.

In clinical diagnosis, EEG and ECG are more important than EOG and EMG. EEG analysis is widely used in monitoring and diagnosis, such as infants monitoring and epilepsy diagnosis. ECG analysis is useful to predict cardiac diseases and to investigate the autonomic nervous system since heart rate variability (HRV) analysis has become a popular tool [11]. The relationship analysis between EEG and ECG are important to understand the mechanisms of human brain and heart in future. However, there are no correlative researches being reported.

Artifact contamination problem is inevitable during the real clinical recording process. EEG and ECG are easy to be contaminated by various artifacts, which may be caused by loosing electrode, eye movement, blink, muscle activity, sweating, deep breath, or movements of head or body. Such artifacts would lead to mis-interpretation results. In order to obtain reliable results, only available signals should be used for either visual inspection or automatic analysis.

For short-term neuro-biological signals analysis, available signals can be selected by visual inspection [15]. For long-term EEG recording, such as sleep data analysis, intensive care unit (ICU) monitoring, and cardiac disease monitoring, it is hard and

laborious to check the artifacts by visual inspection. On the other hand, visual inspection is difficult for unskilled clinicians. In order to obtain reliable results and reduce the heavy burden of visual inspection, automatic artifacts detection and data classification for EEG and ECG are necessary to be developed.

Many papers reported artifacts detection/removal method for EEG and ECG analysis [12]-[14],[16]-[23]. Various advanced methods have been applied to detect and remove artifacts in EEG signals, such as independent component analysis (ICA) [16]-[19], support vector machine (SVM) [17], wavelet analysis [20] and autoregressive (AR) model [21]. These methods were appropriate for offline analysis. For real-time application, the artifact detection algorithms need to be simplified. Agarwal et al. reported an approach of automatic analysis of segmented-EEG [22]. The authors applied a multi-level artifact rejection method during long-term recording. Durka et al. presented an automatic artifact detection system for polysomnographic (PSG) recordings [23]. However, these artifacts detection/removal methods seldom discriminated the artifacts in details. The importance of artifact detection for HRV analysis was emphasized by Berntson et al. [12]. Xu et al. proposed an automatic detection method for HRV analysis [13]. Sapoanikov et al. also presented artifact removal method for ECG [14]. In those methods, only heart beat interval series were considered. Until now, few research results have been reported regarding to the data classification method concerning both EEG and ECG for real-time application.

In this chapter, a model of real-time data classification for EEG and ECG analysis is proposed. Kinds of advanced algorithms, such as ICA [16]-[19], SVM [17], fuzzy cluster analysis [117], self organizing maps (SOM) [118] and group sequential analysis [119], have been used for data classification. But they are not proper for real-time detection. In order to be integrated into the real-time application, the artifact detection algorithm should be significantly simplified comparing with offline detection methods. As an example, the model is applied on a physical system for analyzing the relationship between characteristics of EEG and ECG signals. At first, the artifacts in EEG and ECG were automatically detected. The artifacts detection method was newly constructed based on our previous work [120]. The quality of the signals was then evaluated based on detected artifacts by adjusting weight coefficients according to clinical interpretation purposes. Finally, the evaluated signals were classified by thresholds which were adaptable to clinical interpretation purposes. With the developed real-time system, the quality of signals could be monitored during the recording process, which would be helpful to obtain satisfactory recording and better understanding of artifacts. The proposed data classification method can also be extended for various research purposes by selecting artifacts for removal, defining weight coefficients, and adjusting thresholds.

2.2 Methods

2.2.1 Outline of data classification algorithm

The experimental paradigm is shown in Fig. 2.1 (a). The task environment should be designed according to the purpose of neuro-biological signals interpretations. The measurement equipment records neuro-biological signals when subjects perform the tasks. The recorded data are sent to the real-time data classification system. In this chapter, task environment, subjects, and measurement equipment are explained in section 2.2.2.

Fig. 2.1 (b) illustrates the flowchart of the real-time data classification system. First of all, neuro-biological signals are received from the measurement equipment, filtered for parameter calculation, and segmented for real-time detection. After that, all the parameters are calculated for artifact detection. Artifacts are then detected according to the neuro-biological signals interpretation purpose. Finally, the signals are scored with given weight coefficients and classified by using adaptive thresholds. The weight coefficients and adaptive thresholds are determined by the interpretation purpose of data analysis.

The model of the real-time data classification system can be applied to EEG and ECG analysis. In the following sections, the model will be explained with a physical system and an experiment. The purpose is to analyze the relationship between characteristics of EEG and ECG during long-time mental calculation and rest.

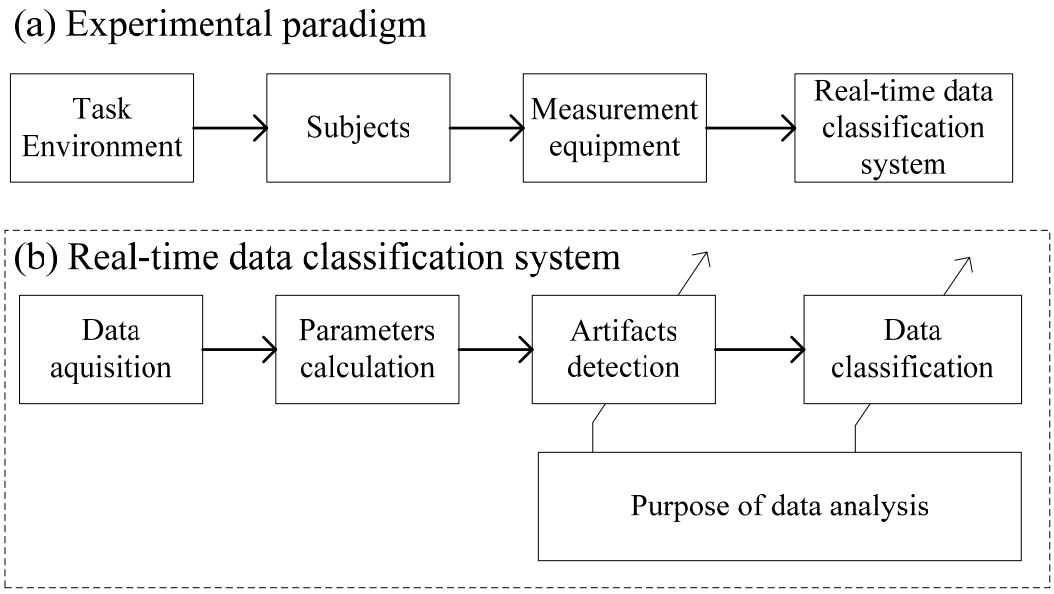

Fig. 2.1 Flowchart of experiment paradigm and real-time data classification system

2.2.2 Data acquisition

2.2.2.1 EEG and ECG data.

The EEG data investigated in this research were recorded from eight healthy male adults, aged 22-25 years old, from System Control Laboratory, Saga University of Japan. The subjects were informed to abstain from alcohol and caffeine 24 hours before experiment. They were requested to have a good sleep at the last night. During the data recording, the subjects were settled in a quiet electrical shield room with the temperature of 24~26 ℃. All the experiments started at 10:00 AM. The subjects gave their informed consent prior to the experiments.

EEG electrodes were placed on the scalp according to the international 10-20 system at the following areas: F_{P1}, F_{P2}, F_3, F_4, O_1, O_2 against ipsilateral earlobe electrode (A_1 or A_2), and F_Z, C_Z against the average of A_1 and A_2 (A_{av}). A pair of ECG electrodes was placed according to standard limb lead II, in order to obtain the largest amplitude of R peak. The electrical impedance was kept under 10 kOhms for all electrodes. EEG and ECG signals were recorded on a digital electroencephalograph (Nihon-Koden EEG 2110) with the sampling frequency of 200 Hz, the upper cut-off frequency at 60 Hz, and the lower cut-off frequency at 0.016 Hz.

2.2.2.2 Experiment tasks

Experiment tasks consisted of four sequential sections: (1) normal rest for 5 minutes; (2) mental calculation for 120 minutes; (3) music relaxation for 15 minutes; and (4) mental calculation for 30 minutes. In mental calculation tasks (section 2 and 4), the subjects had to complete math sums (for example, 63+74) and input answers with a numeric key pad as correctly as possible. The two 2-digit random numbers appeared on a 17 inches computer monitor. In the third section (music relaxation), Mozart Eine Kleine Nachtmusik was used. Subjects were free to open or close their eyes when they were listening to music with an earphone.

2.2.3 Artifacts contamination

Since subjects were not requested to keep still, several kinds of physical activities occurred during recording process. The observed artifacts in EEG and ECG data were explained respectively as below.

2.2.3.1 EEG data

During the long-time task, subjects were too tied to keep still all the time. They

preferred to change postures for comfort. Since body movement affected the potential of all the EEG electrodes, base-line drift and electrode artifact were considered.

The most frequent EOG artifacts were blink and eye movement, which affected the potential of frontal electrodes. During the mental calculation task, subjects kept eyes open. Therefore, blink and eye movement artifacts happened frequently. During rest, subjects closed eyes. There were seldom blink and eye movement artifacts.

EMG artifacts were serious for EEG analysis. When subjects felt uncomfortable and moved their head or neck, EMG artifacts would appear at occipital electrodes. If large EMG artifacts occurred, all the EEG electrodes would be contaminated.

2.2.3.2 ECG data

The body movement is the major reason of artifacts in ECG. EMG artifacts were common in ECG studies, which could be caused by sudden body movements. RR intervals (beat to beat interval series) were the most important information for HRV analysis. The distortion of RR interval including base-line drift and R peak missing was considered as one kind of artifact. The base-line drift was induced by slow body movements. R peak missing was caused by large variability of electrode impedance, which was also caused by body movements.

2.2.4 Parameters calculation

2.2.4.1 EEG data

Four parameters are employed for artifacts detection in EEG: (a) amplitude (μV): $A_z(x)=6\sqrt{S_z(x)}$; (b) symmetry (%): $P_z(x,y)=6\sqrt{S_z(x-y)}/6\sqrt{S_z(x+y)}\times 100$; (c) extension (%): $E_z(x,y)=6\sqrt{S_z(y)}/6\sqrt{S_z(x)}\times 100$; and (d) correlation: $R(x, y)$, where x and y represent specific electrodes of F_{P1}, F_3, O_1, F_{P2}, F_4, O_2, F_Z, and C_Z; z denotes respective EEG component: L (0-0.5 Hz), δ (0.5-4 Hz), θ (4-8 Hz), α (8-13 Hz), β(13-25 Hz), and H (35-50 Hz). The following items are employed in the definition:

- $S_Z(x)$ is the summation of periodogram with the frequency band of z in channel x;
- $S_Z(x\text{-}y)$ is the summation of periodogram with the frequency band of z in channel x and y, in which the EEG time series of channel y is subtracted from that of channel x;
- $S_Z(x+y)$ is the summation of periodogram with the frequency band of z in channel x and y, in which the EEG time series of channel y adds that of channel x.

2.2.4.2 ECG data

Three parameters are employed for artifacts detection in ECG: (a) RR interval series: $y(n)$, (b) estimation of base-line drift: E_{BLD}, and (c) amplitude: A_{H2}. E_{BLD} and A_{H2} are calculated by equation (2.1) and (2.2), where $x(n)$ represent the base-line estimated by a discrete Fourier transform (DFT) low pass filter with a upper cut-off frequency of 1 Hz; H2 denotes high frequency band of (45-59 Hz) and (61-100 Hz); and S_{H2} is the summation of frequency component of H2 band.

$$E_{BLD} = \max\{x(n)\} - \min\{x(n)\} \tag{1.1}$$

$$A_{H2} = 6\sqrt{S_{H2}} \tag{1.2}$$

2.2.5 Artifacts detection

2.2.5.1 EEG data

The criteria for artifacts in EEG are shown in Table 2.1. The left column is the type of artifacts in EEG, and the right column is the judgment condition respectively. The combinations of four parameters defined in section 2.2.4.1 among the EEG channels are utilized for artifact detection in EEG data.

The electrode artifact indicates the ear-lobe reference electrode artifact. Since it is mainly caused by the impedance variety of the reference electrode, electrode artifact would only affect the channels at the same site. If the waveforms are similar in all the adjacent channels on the same site but different with the other site, the related electrode artifact will be discriminated [120]. Left and right sites are discriminated respectively. δ band is employed to detect the oscillation at each channel, and correlation coefficients are employed to judge the similarity between waveforms of different channels. In order to detect the electrode artifact, at least three pairs of electrodes are required. Here, (F_{P1}, F_{P2}), (F_3, F_4), and (O_1, O_2) are employed.

The base-line drift artifact is a type of electrode artifact. The main reason is the variety of electrode impedance, which could be brought by body movement or sweating. Since the impedance variety caused by body movement is slow, L band is employed to judge the oscillation at each channel. Correlation coefficient is used to judge the similarity between the channel pairs on both site of the scalp. If all the conditions are satisfied, base-line drift will be discriminated. For detecting base-line drift artifacts, the electrodes for detecting electrode artifacts are utilized.

Blinks and eye movements are frequent while eyes open. They affect frontal electrodes (F_{P1} and F_{P2}) seriously. The power of low frequency components (A) is employed to detect the oscillation at F_{P1} and F_{P2}. Since left and right eyes blink

together, the symmetry (P) is employed to judge the similarity between F_{P1} and F_{P2}. Because the central region is also affected at the same time, the extension to central region (E) is employed to judge the influence on F_3 and F_4. Based on visual inspection of the waveforms contaminated by blink and eye movement, δ band is selected to discriminate blink, and L band is selected to discriminate eye movement. F_{P1}, F_{P2}, F_3, and F_4 are essential for detection of blink and eye movement.

EMG artifacts are detected respectively for each electrode. The power of H band and β band are used for judgment [120].

Table 2.1 Criteria for artifacts in EEG

Artifacts	Judgment conditions
Electrode	Left: $\begin{cases}\min\{A_\delta(F_{P1}), A_\delta(F_3), A_\delta(O_1)\} \geq 25\mu V,\\ \min\{R(F_{P1}, F_3), R(F_3, O_1), R(O_1, F_{P1})\} > 0.9,\\ \min\{R(F_{P1}, F_{P2}), R(F_3, F_4), R(O_1, O_2)\} < 0.8.\end{cases}$
	Right: $\begin{cases}\min\{A_\delta(F_{P2}), A_\delta(F_4), A_\delta(O_2)\} \geq 25\mu V,\\ \min\{R(F_{P2}, F_4), R(F_4, O_2), R(O_2, F_{P2})\} > 0.9,\\ \min\{R(F_{P1}, F_{P2}), R(F_3, F_4), R(O_1, O_2)\} < 0.8.\end{cases}$
Base-line drift	$\begin{cases}\min\{A_L(x)\} \geq 60\mu V,\\ \min\{R(F_{P1}, F_{P2}), R(F_3, F_4), R(O_1, O_2)\} > 0.8\end{cases}$
Blink	$\begin{cases}\min\{A_\delta(F_{P1}), A_\delta(F_{P2}), A_\delta(F_{P1}+F_{P2})/2\} > 40\mu V\\ P_\delta(F_{P1}, F_{P2}) < 55\%\\ \max\{E_\delta(F_{P1}, F_3), E_\delta(F_{P2}, F_4)\} \leq 85\%\end{cases}$
Eye movement	$\begin{cases}\min\{A_L(F_{P1}), A_L(F_{P2}), A_L(F_{P1}+F_{P2})/2\} > 60\mu V\\ P_L(F_{P1}, F_{P2}) < 55\%\\ \max\{E_L(F_{P1}, F_3), E_L(F_{P2}, F_4)\} \leq 85\%\end{cases}$
EMG	$\begin{cases}A_H(x) \geq 10\mu V,\\ A_H(x) \geq A_\beta(x)\end{cases}$

*The thresholds are established for the recording filtered between 0.53 Hz and 60 Hz.

2.2.5.2 ECG data

The criteria for artifacts in ECG are shown in Table 2.1. The left column is the type of artifacts in ECG and the right column is respective judgment conditions. The three parameters defined in 2.2.4.2 are utilized for artifact detection in ECG data.

RR intervals (beat to beat interval series) are between 0.4 and 1.2 seconds for normal people in quiet status. Abnormal RR intervals should be rejected for HRV analysis. This kind of distortion of interval is large. The large base-line drift reflects body movements or deep breathing, which indicates that ECG signals contain the information of physical activities. If the large base-line drift is detected, it is not proper to analyze the relationship between ECG signals and mental activity. However, HRV could be correctly calculated. This kind of distortion of interval is small.

The power of high frequency components is employed to identify EMG artifacts. If the power is larger than 200 μV, which may affect R peak detection, large EMG artifacts will be determined. If the power is larger than 58 μV, which indicates that ECG signals include the information of physical activities, small EMG artifact will be determined.

Table 2.2Criteria for artifacts in ECG

Artifacts	Level	Judgment conditions
Distortion of interval	large	$y(i)$>1.2 s, or $y(i)$<0.4 s
	small	E_{BLD}>900 μV
EMG artifacts	large	$A_{H2}(x)$>200 μV
	small	$A_{H2}(x)$>58 μV

*The thresholds are established for the recording filtered between 0.08 Hz and 60 Hz.

2.2.6 Data classification

According to the purpose of data analysis, weight coefficients are given to the artifacts for quality evaluation of each segment. The segments are then scored on the basis of detected artifacts.

The score of EEG or ECG is equal to the summation of the weight of detected artifacts. The score will be revised as 1, if larger than 1. 0 stands for the best signals, and 1 for the worst. The weight coefficients for all the artifacts are shown in Table 2.3.

Table 2.3 Weight coefficients for quality evaluation

Artifacts in EEG		Weights
Electrode		0.1
Base-line drift		0.1
Blink		0.1
Eye movement		0.1
EMG artifacts		0.1
Artifacts in ECG		Weights
Distortion of interval	large	1.0
	small	0.5
EMG artifacts	large	1.0
	small	0.3

A weight of 0.1 is given to the artifacts in EEG. Since EMG artifact is detected respectively for each channel, the total weight of 8 channels is 0.8. A weight of 1.0 is given to large distortion of interval and large EMG artifacts. A weight of 0.5 is given to small distortion of interval. A weight of 0.3 is given to small EMG artifacts. At last, the segments are scored by the higher score of EEG and ECG, and are classified as

three groups (best, available, and worst) by two given thresholds for the best and the worst. In this chapter, the segments will be classified as the worst for a score larger than 0.7, and the best for a score less than 0.2.

2.2.7 Real-time realization by DA-AD converter

The whole algorithm was realized in real-time. The data classification system received the signals from the digital electroencephalograph through a DA-AD converter. EEG signals (channel 0-7) were transferred with the lower cut-off frequency at 0.53 Hz, and ECG signals were transferred with the lower cut-off frequency at 0.08 Hz (channel 8). The recording was divided into 5.12 s segments. The algorithm was repeated for each segment.

The interface contains the following items: 1) subject information, 2) original waveforms, 3) detected artifacts, 4) history trends of selected artifact, and 5) history trends of total score. By these items, the quality of recording can be properly estimated. In order to obtain satisfactory recording, when unexpected artifacts were detected, the user should find out the origin as soon as possible. If the artifacts were induced by physical activities, the user should remind subjects to keep still. If the artifacts came from equipment such as loose electrode, the experiment might have to be paused and performed again.

2.3 Results

2.3.1 Real-time data classification

The interface of real-time data classification system is shown in Fig. 2.2. Part A is subject information. Part B shows time series of three continuous segments. Detected artifacts are listed in Part C. The notation “YES” denotes *detected*, while blank denotes *not detected*. In the line of *EMG artifact (EEG)*, the number below “YES” is the amount of detected channels. Part D illustrates the history trends of selected artifact events, which could be changed with the menu button of History. Part E displays the history trends of total weights. The upper dashed is the threshold of 0.7 for the worst signals, and the lower is the threshold of 0.2 for the best.

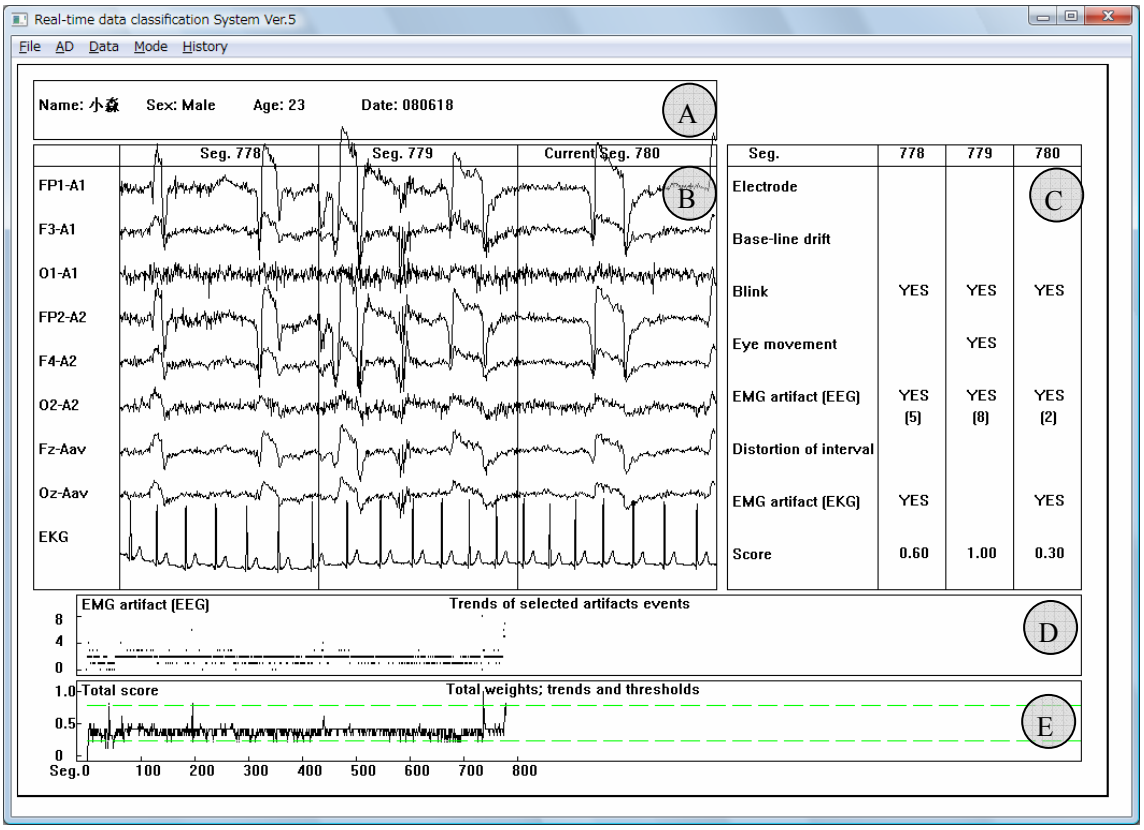

Fig. 2.2 The interface of real-time data classification system

2.3.2 Effect of data classification

The power of α band (A_α) and the power of β band (A_β) are common characteristics in EEG analysis. Heart rate (HR), power of low frequency components (LF) and high frequency components (HF) are common for ECG analysis. As an example, A_β(F4) and HR are used to analyze the relationship between EEG and ECG.

As shown in Fig. 2.3, the relationships between A_β(F4) and HR are analyzed by three different data selection method. Although all the recordings form eight subjects were analyzed by real-time data classification system, only the results of two subjects are shown in Fig. 2.3. The horizontal axis indicates EEG parameters of A_β(F4). The vertical axis indicates the ECG parameters of HR. As shown in Fig. 2.3 (a), 263 segments from subject A and 152 segments from subject B, whose score is less than 0.2, are selected as the best segments by proposed selection method. As shown in Fig. 2.3 (b), 124 segments from subject A and 124 segments from subject B, whose segment number can be exactly divided by 20, are selected as random segment. As shown in Fig. 2.3 (c), 202 segments from subject A and 65 segments from subject B, whose score is larger than or equal to 0.7, are selected as the worst segments by

proposed selection method. With proposed selection method, the best segments are clustered, while the worst segments are scattered. Additionally, a few randomly selected segments are scattered from the others.

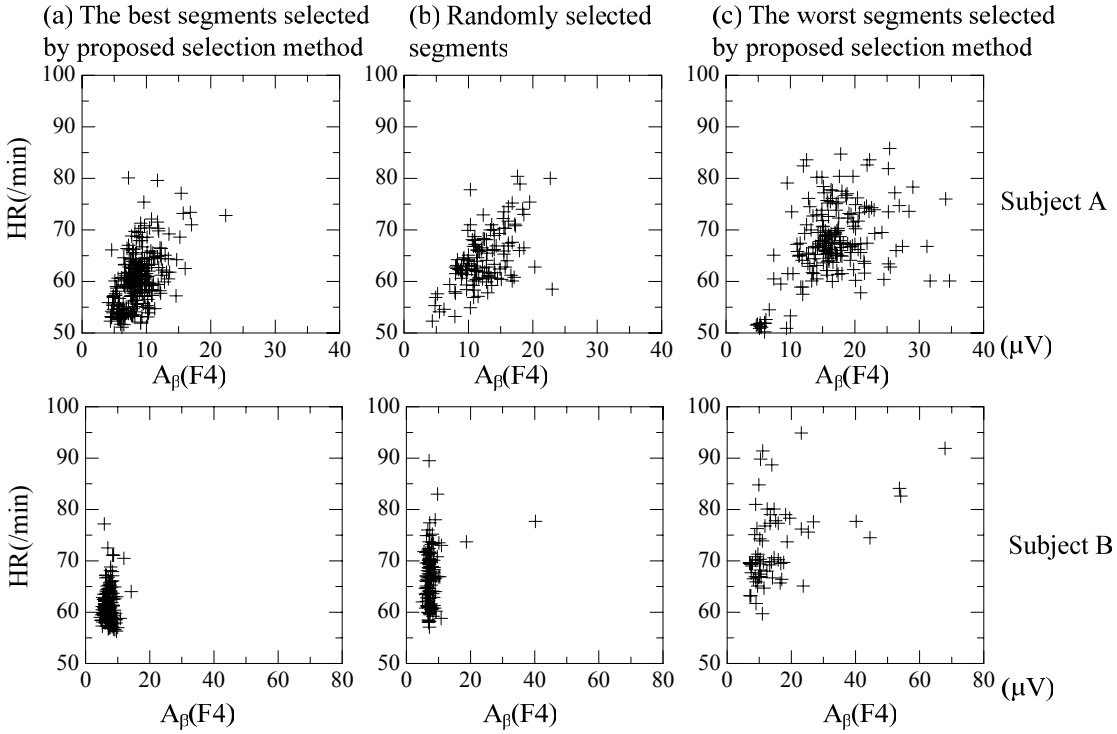

Fig. 2.3 The comparison of relationship analysis between EEG and ECG parameters with different data selection method

2.4 Discussion

2.4.1 Weight coefficients

2.4.1.1 Weight setting

The weight coefficients for each artifact should be given properly according to the purpose of data analysis, which determines the importance level of contaminated information. During the EEG data analysis, frequency components of δ, θ, α, and β are mostly studied. In addition, the information of α band and β band is more important than that of δ band and θ band. During the ECG data analysis, continuous RR intervals are the most important information for HRV interpretation.

Ear-lobe reference electrode artifact, base-line drift, blink, and eye movement affect low frequency components (usually δ band, sometimes θ band, seldom α band). Although blink and eye movement can be frequently encountered when eyes open, but

both of them only affect the frontal electrodes. Therefore, all these four artifacts are given a low weight of 0.1.

EMG artifacts affect both EEG and ECG signals. For EEG analysis, EMG artifacts increase the power of β band seriously and sometimes also increase the power of α band. For ECG analysis, small EMG artifacts indicate possible physical activities, so that the signals are not proper for mental activity analysis; large EMG artifacts may induce wrong detection of R peak, which are not available for HRV analysis. Therefore, a total weight of 0.8 was given to EMG artifacts in EEG, a weight of 0.3 was given to small EMG artifacts in ECG, and a rejection weight of 1.0 was given to large EMG artifacts in ECG.

Large distortion of interval indicates interrupted RR intervals, which is caused by false or miss detection of R peak. Small distortion of interval indicates that RR intervals contain the information of not only mental activities, but also physical activities. Physical activities could be reflected by large base-line drift of ECG signals. Therefore, a rejection weight of 1.0 was given to large distortion of interval, and a weight of 0.5 was given to small distortion of interval.

2.4.1.2 Extended application

In this research, the purpose of experiment is to study the relationship between characteristics of EEG and ECG, i.e. both EEG and ECG signals are important, so that the final score is defined as the higher score of EEG and ECG.

Users should define all possible artifacts according to analysis purposes, and adjust the weight coefficients according to the importance of the information contaminated by corresponding artifacts. After that, users should define the score and adjust the thresholds for data classification for their own analysis purposes. For example, if the purpose is to analyze the characteristics of EEG, a weight of 0 should be given to the artifacts in ECG. If the purpose is to analyze the characteristics of ECG under certain physical activity, small EMG artifact and small distortion of interval, both of which contain information of physical activities, should not be considered as artifacts any more, and a weight of 0 should be given.

Moreover, the recording conditions are crucial for artifacts detection. The recording conditions presented in section 2.2.2 and 2.2.7 are common in clinical analysis. The criteria illustrated in section 2.2.5 are established under these conditions. The criteria should be adjusted to recording conditions in different experimental paradigm for the individual analysis purpose. The principles for judgment of each artifact are described in section 2.2.5. The criteria are allowed to be revised according to the principles. For instance, in order to identify electrode artifacts, at least three pairs of electrodes should be recorded. In this chapter, (F_{P1}, F_{P2}), (F_3, F_4), and (O_1, O_2) are utilized. If O_1 and O_2 are not recorded, but T_3 and T_4 are recorded, then (F_{P1}, F_{P2}), (F_3, F_4), and (T_3, T_4) are also effective. On the other hand, some artifacts may not be

able to be detected under certain recording conditions because of lacking information, e.g. blink will not be detected except all the necessary channels (F_{P1}, F_{P2}, F_3 and F_4) are recorded.

2.4.2 Effect of data classification

The difference between the best and worst segments classified by proposed data classification method is obvious, as shown in Fig. 2.3 (a) and (c). The worst segments include seriously contaminated signals. Most artifacts are caused by body movement, which could increase the power of β band in EEG, and affect the heart rate. That is the reason why the worst segments are scattered.

The quality of the recording for analysis is crucial for obtaining reliable characteristics. If the worst segments are used for data analysis, the accuracy of the results will be seriously affected, as shown in Fig. 2.3. The best segments, which are selected by proposed data classification method, represent stable characteristics. The characteristic of randomly selected segments is disturbed by a few bad segments. The characteristic of the worst segments is vague. The presented data classification method is effective for meaningful analysis.

2.4.3 Real-time application

Artifacts detection is crucial for reliable analysis of EEG or ECG signals. However, in most research work, the artifacts are usually detected after recording. Therefore, it is very difficult to find out the actual reason. Moreover, for long-time experiment, it is necessary to monitor the quality of signals in real-time, in order to obtain satisfactory recording. If continuous serious contamination is detected after recording, long-time experiment has to be performed again. In this chapter, a data classification method is developed for real-time application. The major part is artifacts detection algorithm. Most papers reported artifacts detection methods with offline mode [16]-[21]. They used complicated algorithms to detect or separate artifacts from original signals. But our research aims to obtain satisfactory recording, and provide available data for offline analysis. Therefore, our artifacts detection algorithm is significantly simplified comparing with others. With the model and artifacts detection algorithm, the user could monitor the recording quality in real-time, and perceive contaminated signals promptly. It is also possible to find out the reason of artifacts during recording process.

2.5 Conclusions

In this chapter, a real-time data classification model for accurate analysis of neuro-biological signals was proposed. As an example, a physical system to analyze the relationship between characteristics of EEG and ECG was developed. The results suggested that the proposed data classification method was effective. Comparing the best and worst segments, it was observed that contaminated signals would lead to mis-interpretation. With this system, it is convenient to monitor the quality of signals, acquire better understanding of artifacts, and obtain satisfactory recording.

Chapter 3

An automatic spike detection system based on elimination of false positives using the large area context in the scalp EEG

3.1 Introduction

The electroencephalogram (EEG) has been an important tool in epilepsy diagnosis. The EEG waveforms related to epilepsy are often characterized as epileptiform, spike or sharp-wave. Most researchers use the definition of spike given by Chatrian et al. in 1974: "a transient, clearly distinguished from background activity, with pointed peak at conventional paper speeds and a duration from 20 to under 70 ms, i.e., 1/50 to 1/14 s, approximately. Main component is generally negative relative to other areas. Amplitude is variable." [24] Sharp wave is with a duration from 70 to under 200 ms. The definition is too simple to differentiate spike activities from other EEG activities such as alpha waves, electromyogram (EMG) artifacts, blinks, and other abnormal EEG activities. Researchers find that most spike activities appearing in multichannels are followed with slow waves, and have explicit focuses. Traditionally, the EEG recording is visually scanned by an experienced electroencephalographer (EEGer). In recent years, along with the development of computer technology, long-term recordings have been widely used. Traditional visual inspection of long-term recordings is time-consuming. Therefore, automatic detection is necessary. Over the past 30 years, a number of automatic spike detection methods have been developed, such as mimetic method [33], [36], contextbased system [51], [52], expert system [53], template method [89], [91], artificial neural network [63], [68], [69], wavelet analysis [71], [77], support vector machine [121], morphological

filter [100], Kalman filter [94], [95], independent component analysis [92], [93], fuzzy C-means [108], deterministic finite automata [110], association rules [122], multi-stage and multi-method system [54] [55] [79]–[81], and so on. The reviews in detail can be referred to [25] [28]–[32].

Even with advanced algorithms, there are still many false positives (FPs) [30], [32]. False detections decreased the confidence of clinicians in automatic detection [113]. Most researchers assessed FPs by selectivity and false positive rate, while only a few directly utilized the characteristics of FPs for elimination of FPs, such as Gotman et al. [33], [36], Glover et al. [51], [52], Jones et al. [53]-[55], Liu et al [79], and Argoud et al. [81]. Most papers naturally concentrated on the characteristics of "spikes", while that of "false positives" have not been given sufficient attention, as well as focus, which is an important characteristic of spike activities. In the case of the common average reference (AV) montage, focus is used for definition of focus electrode: the channel with maximum negative peak. In the case of the bipolar (BP) montage, phase reversal between two channels is commonly used. However, the information of other channels has not been fully utilized. Moreover, the slow-wave part is not employed in most of the methods. The reason may be that the morphology of the slow-wave part varies more greatly than that of sharp transients [79]. But the slow-wave part is as important as the spike part in both clinical diagnosis and automatic detection.

The co-authors had developed an automatic EEG interpretation (AEI) system [123], [124]. In this chapter, we designed a spike detection system for the AEI system. A preliminary version of this work was reported in Japanese [125]. We attempted to answer "what is not a spike" rather than "what is a true spike". Large area context available on 49 channels from two common montages were used. The FPs from typical artifacts were identified by analyzing the morphology and power spectrum of the background activities in single channel. The FPs from other EEG activities were differentiated by the characteristics of spike activities: 1) spike activities could be observed with at least two electrodes; 2) spike activities should show clear focus characteristics in BP montage; 3) in the whole recording, only the focus channels with frequent sharp transients were effective. Finally, a multi-channel template method was applied to confirm true spike activities.

3.2 Methods

3.2.1 Subjects and data acquisition

EEG signals were recorded by a digital electroencephalograph (Nihon-Koden EEG2100) in the Kyoto University Hospital. Twenty-one electrodes including

ear-lobes were placed according to the international 10-20 system [1]. The EEG signals were recorded with a sampling frequency of 200 Hz and band-pass filtered by 0.016-120 Hz using hardware. The electrodes were referenced to a common referential electrode. The signals could be reformatted as any montages later.

17 recordings were recorded from 17 patients (29-69 years old). The recordings ranged from 3 to 55 min, 478 min in total. They were also used in the previous work [125]. Visual inspection of the recordings was done by qualified EEGers. Spike activities were observed in the recordings from 6 epilepsy patients, which were named as S1-S6 respectively. S1 had occasional high amplitude spikes on the right hemisphere; S2 had occasional spikes on the right posterior quadrant; S3 had occasional focal spikes on the right midtemporal; S4 had frequent high amplitude spikes on the right, and occasional on the left; S5 had paroxysmal bursts of high amplitude spikes more on the left; and S6 had spikes on the left and right. The other 11 patients with other disorders were considered as a whole, and named as NS.

3.2.2 Block diagram

As shown in Fig. 3.1, the system consists of three stages. 1) The AV montage stage created candidate spike events by detecting AV channels. All the transients which were possible to be spikes were picked out. Artifacts were examined for each transient. Then the remained transients were grouped as events by spatial and temporal relations. 2) The BP montage stage aimed at focus analysis for each event. Possible BP spikes were detected by a template method with adaptable durations. The focus channel was identified by a "weighting method" integrating the information (polarity, amplitude and distribution) of all BP spikes. 3) The template stage was taken from a viewpoint of the whole recording. Events were clustered by focus channels. The multi-channel template was extracted only for the focus channels with sufficient events. Finally, a set of simple rules were used for template matching. Elimination of FPs was carried out in all the stages. In the AV montage stage, typical artifacts and the events with single AV sharp transient were removed. In the BP montage stage, the events without focus were deleted. In the template stage, the events with ineffective focus channels were ignored.

Since no spike activities were identified before template matching, all detections in single channel were named as sharp transients (STs). An ST event consisted of a few AV STs and BP STs. The spike activities in single channel including spike, sharp-wave, spike-and-wave, and sharp-and-wave, were abbreviated as spikes, and in multi-channel as spike events.

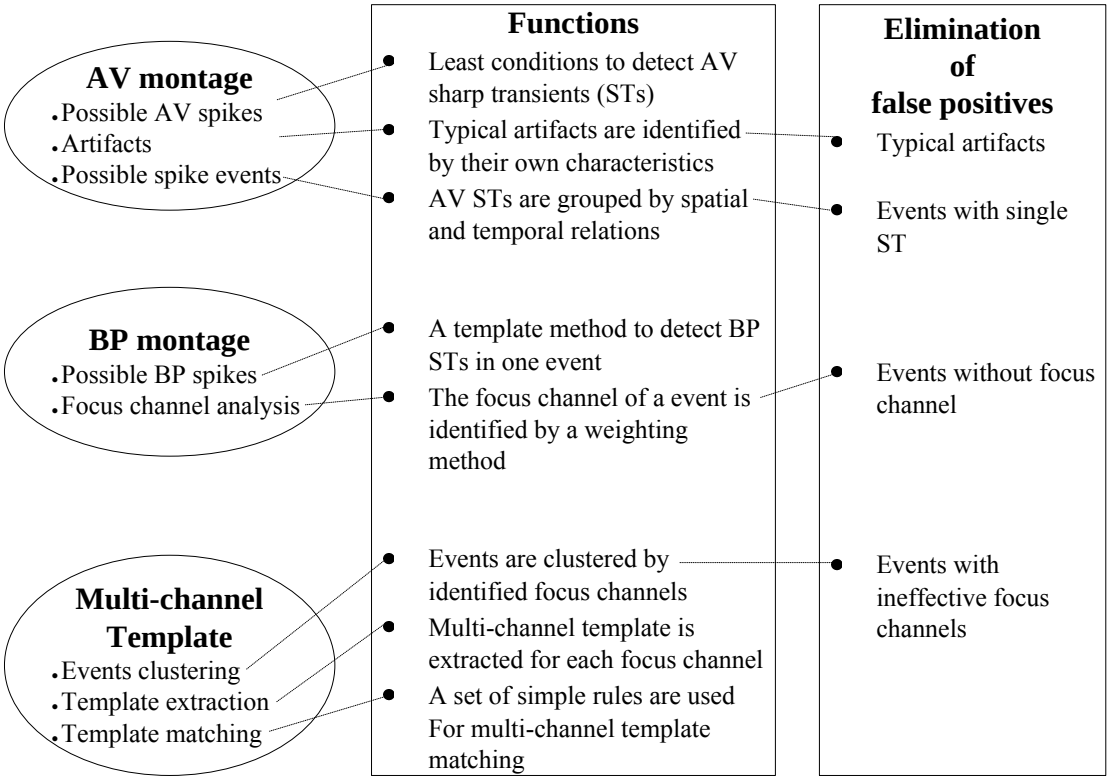

Fig. 3.1 Block diagram of the spike detection system. The AV montage stage created possible spike events. The BP montage stage emphasizes focus analysis. The template stage surveys the results from a viewpoint of the whole recording. False positive detection is carried out in all stages.

3.2.3 AV montage

Except for ear-lobes, 19 AV channels were derived. Each electrode was referenced to the average potential of all 19 electrodes. Since there is no focus around FZ, CZ and PZ, we only detected the other 16 channels.

Before detection, all the AV channels were filtered by a digital band-pass filter of 0.53-20 Hz. The upper cutoff frequency of 20 Hz was used to attenuate fast activities and reduce calculation burden. 20 Hz was a trade-off between amplitude and calculation efficiency, i.e. a lower one decreased the amplitude of spike severely, while a higher one remained many fast activities. Besides, the signals were segmented for every 5.12 s, which could provide a frequency resolution of 0.2 Hz. From previous study, this resolution was accurate enough for estimation of background activities [123], [124]. The power spectrum was estimated by applying a rectangular window with fast Fourier transform (FFT) over each channel in each segment.

3.2.3.1 Possible AV spikes

A typical ST is shown in Fig. 3.2. Five key peaks and four half-waves are defined. The definition was developed based on previous work [125]. For each half-wave, the amplitude and duration were calculated. Additionally, the amplitude of an ST (AST) was defined as the average of AS1 and AS2. In the following text, we define spike-and-wave (SW) duration as from P1 to P3, and spike-only (SO) duration as from P1 to P2. In order to include all possible spikes by detecting AV STs, three categories were employed: "clear" spike with or without slow wave, "small" spike with at least "small" slow wave, and "vague" spike with "clear" slow wave. The least conditions are shown in Table 3.1. The conditions were used to collect candidates, not to identify spikes.

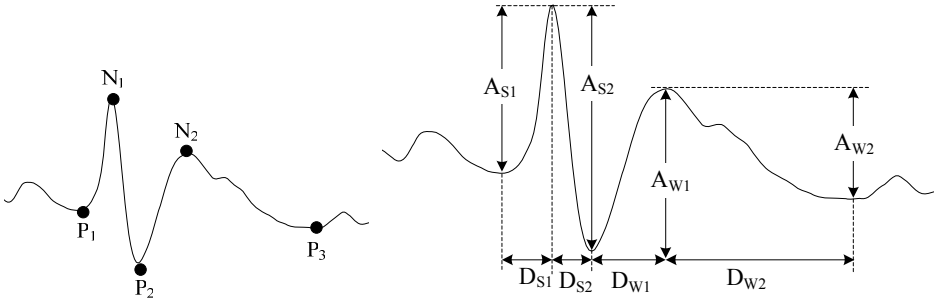

Fig. 3.2 Parameters for detecting STs. Five key peaks and four half-waves (*P*1*N*1, *N*1*P*2, *P*2*N*2 and *N*2*P*3) are defined. For each half-wave, the amplitude and duration are computed.

Table 3.1 Least conditions for detecting AV STs

Parameter	Conditions		
(Spike)	Clear	Small	Vague
A_{S1}[μV]	>30	>20	
A_{S2}[μV]	>50	>40	
max{D_{S1}, D_{S2}}[s]	<0.13	<0.13	<0.13
(Slow wave)	Vague	Small	Clear
min{A_{W1}, A_{W2}}[μV]			>40
D_{W1}+D_{W2}[s]		>0.15	>0.15
A_{W1}/D_{W1}[μV/s]			>400
A_{W2}/D_{W2}[μV/s]			>260

3.2.3.2 Typical artifacts

For each AV ST, the power spectrum of four epochs (BG 1-4) in Fig. 3.3 (a) was

estimated by applying a rectangular window with FFT. The frequency bands of theta (4-8 Hz), alpha (8-13 Hz), and high (H: 25-100 Hz) were used. The mean power of band *z* for BG *i* was evaluated by

$$A_{zi} = 6\sqrt{S_{zi}} \tag{3.1}$$

where S_{zi} was the summation of power spectrum with band *z* in BG *i*. The minimum and maximum amplitude of band *z* was defined as

$$\begin{cases} A_z^{\min} = \min\{A_{zi}\} \\ A_z^{\max} = \max\{\min\{A_{z1}, A_{z2}\}, \min\{A_{z3}, A_{z4}\}\} \end{cases} \tag{3.2}$$

In order to evaluate the importance of an ST to band *z*, we defined $M_z^{\max}$ and $M_z^{\min}$ as

$$\begin{cases} M_z^{\max} = A_{\mathrm{ST}} / A_z^{\min} \\ M_z^{\min} = A_{\mathrm{ST}} / A_z^{\max} \end{cases} \tag{3.3}$$

Besides, segment background activities of the channel including current AV ST were also evaluated. The mean amplitude of band *z* was defined as A_z^{seg} and computed by (3.1). Then the FPs from typical artifacts were identified by their own characteristics.

Alpha waves. P_α was defined as the largest percentage of $S_{\alpha i}/(S_{\alpha i} + S_{\theta i})$ in BG 1-4. If $P_\alpha > 90\%$, the ST was eliminated directly. If $P_\alpha < 40\%$, the ST was not examined. Along with P_α increased from 40% to 90%, only the STs satisfying $M_\alpha^{\max} > 10 \times (P_\alpha - 0.4)$ were kept for further test.

EMG artifacts. For current segment, if $A_{\mathrm{H}}^{\mathrm{seg}} > 40\mu\mathrm{V}$, the ST was deleted. If $A_{\mathrm{H}}^{\mathrm{seg}} < 40\mu\mathrm{V}$, the ST must stand out from EMG activities: $M_{\mathrm{H}}^{\max} > 4$ and $M_{\mathrm{H}}^{\min} > 3$.

Blinks. We employed six half-waves including four in Fig. 3.2 and another two before *P*1. For each half-wave, if the amplitude was higher than 100 μV, and the ratio of negative amplitude to positive was less than 0.1, the ST was eliminated. Only the STs located at frontal area were examined.

Slow waves. As shown in Fig. 3.3 (b), four parameters were used for shape analysis. The relative sharpness ($S_{\mathrm{S}i}$) was defined as $A_{\mathrm{Sg}i}/A_{\mathrm{S}i}$. If $D_{\mathrm{S}i}<0.1$ s, the ST was examined. Along with $D_{\mathrm{S}i}$ increased from 0.1 s to 0.13 s, an ST was remained only if $S_{\mathrm{S}i} > 0.5 + 10 \times (D_{\mathrm{S}i} - 0.1)$.

Complex channels. It is defined as the AV channel in one segment with high

amplitude alpha and theta waves. The channel was identified only if $\min\{A_\alpha^{\min}, A_\theta^{\min}\} > 25\mu V$ was detected in continuous three segments: previous, current and next. The STs in complex channels must stand out from both alpha and theta waves: $M_\alpha^{\max} + \max\{M_\alpha^{\min}, M_\theta^{\max}\} > 6$.

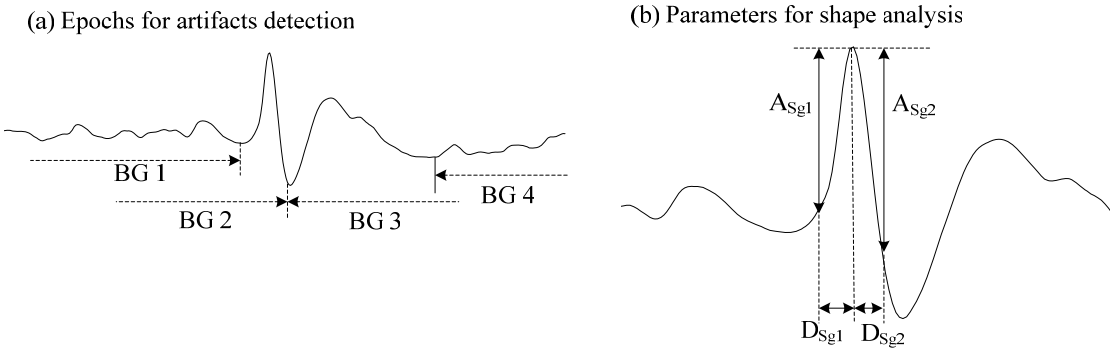

Fig. 3.3 Epochs and parameters for artifact rejection. (a) Four epochs (BG 1-4) each lasting 1.28 s are used. (b) Four parameters (A_{Sg1}, D_{Sg1}, A_{Sg2} and D_{Sg2}) are used for shape analysis to remove slow waves. D_{Sg1}=0.618×D_{S1} and D_{Sg2}=0.618×D_{S2}.

3.2.3.3 Possible spike events

The remained AV STs were grouped as ST events by spatial and temporal relations. Since only the most typical artifacts were rejected, it was expected that all spike events were included. The AV STs, which had the largest *A*ST within 50 ms before and after, were declared as *focus ST*. The other AV STs were grouped to the nearest *focus ST* within 50 ms. An *event pattern* was obtained by averaging the waveforms of focus and adjacent AV STs for each ST event. The ST events only including *focus ST* were eliminated.

3.2.4 BP montage

In this stage, the focus channel was identified for each ST event, and the ST events without focus were eliminated. Thirty BP channels were derived from 19 AV channels.

3.2.4.1 Possible BP spikes

At first, the polarity of a BP channel was identified by a template method using *event pattern*. R_{SW} and R_{SO} denoted the correlations between *event pattern* and a BP channel with SW and SO duration. The SW and SO durations were adaptable to

individual event by detecting key peaks of *event pattern*. If both R_{SW} and R_{SO} were positive, it might be a negative spike; if both were negative, it might be a positive spike; if they were opposite, it could not be a spike.

Table 3.2 Conditions for detecting BP STs

Parameter	State-SW	State-SO
$\lvert R_{SW}\rvert$	>0.35	
$\lvert R_{SO}\rvert$		>0.7
$R_{SW}\times R_{SO}$	>0	>0
A_{ST}^{b}	>20	>20
$\max\{D_{S1}^{b}, D_{S2}^{b}\}$ [s]	<0.13	<0.13
A_{ST}^{b}	$>100\times(1-\lvert R_{SW}\rvert)$	$>200\times(1-\lvert R_{SO}\rvert)$

R_{SW} and R_{SO} are the correlations with SW and SO durations between BP channels and event pattern.
The superscript ^{b} denotes the parameters belong to BP STs.

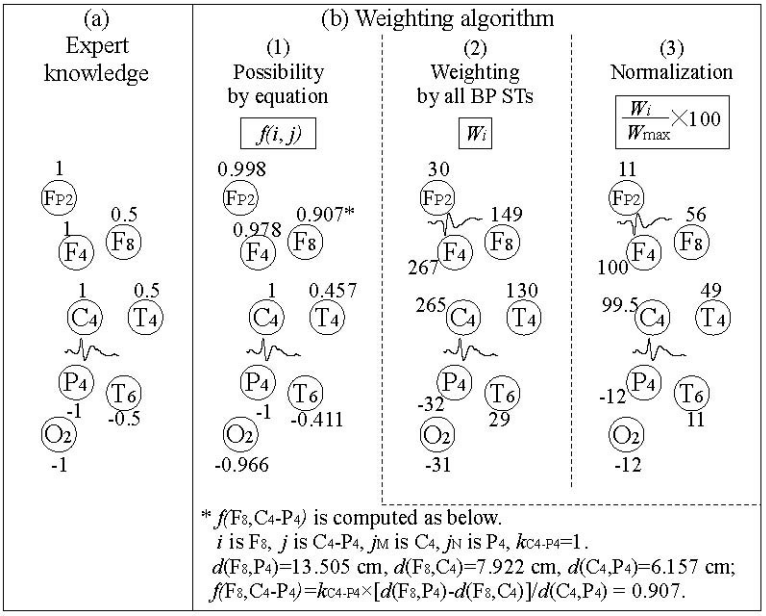

Fig. 3.4 Focus channel identification. (a) Possibilities of being focus contributed from a negative ST in C4-P4 are assessed by expert knowledge. 1 stands for most possible, and -1 for most impossible. (b) A weighting algorithm based on expert knowledge. (b-1) Possibilities assessed by (3.4). Spherical distances are obtained according to international 10-20 system using a head model with a radius of 10 cm. (b-2) Weights assessed by (3.5). Suppose a positive ST is detected in FP2-F4, A_{FP2-F4}=120 μV, A_{C4-P4}=150 μV. (b-3) Normalized weights. $W_{max}=W_{F4}$=267 μV.

Then the key peaks of BP STs were detected according to the polarity. The criteria for detecting BP STs are shown in Table 3.2. A BP ST was declared if at least one state was satisfied. Similar to the conditions in Table 3.1, the conditions here were not for identifying true spikes, but for including all possible spikes to provide enough information for accurate identification of focus channels. Therefore it was necessary to detect all the STs related to spike activities.

3.2.4.2 Focus channel analysis

Experts usually investigate focus channel based on the information from all BP spikes. Based on that knowledge, a "weighting method" was developed. First of all, the possibility of being focus was assessed for each electrode by the information from single BP ST. Suppose a negative ST is detected in *C*4-*P*4. The focus is most possible at *FP*2, *F*4 and *C*4. *F*8 and *T*4 are also possible to be focus, but the possibility is lower. As for *P*4, *O*2 and *T*6, they are impossible to be focus, since spike activities originated from this area will result a positive ST in *C*4-*P*4. If 1 stands for most possible and -1 for most impossible, the possibilities can be assessed as shown in Fig. 3.4 (a). Based on Fig. 3.4 (a), if j is a BP ST in channel j_M-j_N, the possibility of electrode i contributed from j can be assessed by:

$$f(i,j) = k_j \times \frac{d(i,j_N) - d(i,j_M)}{d(j_M,j_N)} \tag{3.4}$$

where k_j is the polarity of j (1 for negative and -1 for positive); $d(i, j_M)$; $d(i, j_N)$, and $d(j_M, j_N)$ are spherical distances between electrodes. The results are shown in Fig. 3.4 (b-1).

Then considering the amplitude of BP STs, the weight of electrode i can be evaluated by the sum of contribution from all BP STs:

$$W_i = \sum_j \{f(i,j) \times A_j\} \tag{3.5}$$

where j is a BP ST, A_j is the average amplitude of j. The weights contributed from two BP STs in *C*4-*P*4 and *FP*2-*F*4 are shown in Fig. 3.4 (b-2).

Finally, if the electrodes X, Y and Z have the largest three weights in order, the focus channel is identified by two steps:

1) Is $W_Y = W_X < 0.8$, and Y is adjacent to X? Yes→the AV channel X-Av is focus channel; No→ 2);

2) Is $W_Z = W_Y < 0.8$, and Z is adjacent to X? Yes→the BP channel X-Y is focus channel; No→X-Av is focus channel.

From the distribution of normalized weights in Fig. 3.4 (b-3), it is easy to identify *F*4-*C*4 as the focus channel.

After the focus channel was identified, the event was examined by the

distribution of AV STs, BP STs, and the focus channel. We defined the electrodes with AV STs as ST electrodes, and others as NST electrodes. An event was kept for further test only if it satisfied the following conditions:
1) All NST electrodes adjacent to ST electrodes were connected to at least one ST electrode by BP STs;

2) $\max\{W_i\} > 240\mu V$ with at least two ST electrodes, or $\max\{W_i\} > 180\mu V$ with at least three ST electrodes;
3) If the focus was an AV channel, it must be an ST electrode; if the focus was a BP channel, both terminal electrodes must be ST electrodes.
Otherwise, the event was declared as no focus and removed.

3.2.5 Multi-channel template

Since BP spikes have two polarities, the template should be of multi-channel. For different focuses, at least the polarities of some BP STs are different. For example, a focus of *T*4 possibly results a positive ST in *F*8-*T*4, while a focus of *F*8 possibly results a negative ST in *F*8-*T*4. Moreover, the variation of spike waveforms in multi-channels possibly has relations with the impedance distribution of the scalp. Since the impedance of the scalp is fixed for the same patient, the spike events originated from the same focus possibly have the similar waveform patterns in multi-channels. Therefore, the multi-channel template was extracted for each focus channel.

3.2.5.1 Event clustering

As the focus channels had been identified, it was convenient to cluster events by their focus channels. The focus channels clustered more than 8 events were declared as effective, others as ineffective. Only the ST events with effective focus channels were kept for further analysis. The events with ineffective focus channels were eliminated.

3.2.5.2 Template extraction

Waveform averaging is reliable to eliminate background EEG activities. We extracted multichannel templates by averaging waveforms twice. For each focus channel, the template was extracted by following procedures.

a) Alignment: All the clustered ST events were aligned on the apex (*N*1) of focus STs.

b) Initial template: The waveforms of the same channel in all ST events were averaged. As a result, the template consisted of 19 AV channels and 30 BP channels.

c) ST channels: The channels detected as STs in more than 75% of total clustered ST events were defined as ST channels.

d) Correlation analysis: The SW duration of averaged waveform of AV ST channels in *initial template* was used. The correlations of *ST channels* between ST events and *initial template* were computed. If the largest correlation was less than 0.7, the ST event was eliminated.

e) Final template: Only if the focus channel remained more than 6 ST events, it was declared as effective. Otherwise, all the events at the focus channel were ignored. Final template was extracted from remained ST events.

3.2.5.3 Template matching

Each effective focus channel had a multi-channel template and at least 6 ST events. For each of them, the SW duration of averaged waveform of AV ST channels in *final template* was used for correlation analysis. The correlations of *ST channels* between each ST event and *final template* were computed. An ST event was declared as a TRUE event, if all the following rules were satisfied:

1) The average correlation was larger than 0.4;
2) The maximum correlation was larger than 0.77;
3) There were at least three correlations larger than 0.7.

However, focus channels may be wrongly identified. For example, if the actual focus was around *T*4-*Av*, but *F*8-*T*4 is not detected as a positive ST for distorted waveforms, then *F*8-*T*4 is identified as the focus channel. In this case, if the event is rejected by the template of *F*8-*T*4 but highly correlated with the template of *T*4-*Av*, it should also be declared as TRUE. In other words, the rejected ST events should be matched with the templates of adjacent effective focus channels. If the template matching rules were satisfied for at least one focus channel, the rejected ST event was clustered to new focus channel, and declared as TRUE.

3.3 Results

3.3.1 AV montage

3.3.1.1 AV STs and typical artifacts

The results of AV montage detection are illustrated in Fig. 3.5. Black and gray dots are detected AV STs. Gray dots denote that the STs were rejected as typical artifacts. As shown in Fig. 3.5 (a), all spikes were detected in normal EEG. In Fig. 3.5 (b), AV STs almost included all negative peaks of α waves in O1-Av, and all were rejected. The α activities in P3-O1 were attenuated, so that the difficulty for

identification of α waves was increased. An example of twice blink is shown in Fig. 3.5 (c). One AV ST was detected in FP2-Av, and eliminated for blinks. Since positive peaks in AV channels were not concerned, only continuous blinks were possibly detected. Many positive STs (circles) must be considered to detect only BP channels. Thus the burden of artifact rejection will be increased. EMG artifacts are included in Fig. 3.5 (d). Most obvious peaks were detected as AV STs and eliminated for EMG artifacts. There were also some STs, which were detected from slow waves or complex channels and rejected by corresponding conditions.

3.3.1.2 ST events

As shown in Fig. 3.5 (a), 10 ST events were detected in normal EEG and marked with arrows and numbers. The results of each stage are illustrated with arrows. Events 2, 5, 7, and 8 corresponding to ST a, b, c, and d, were eliminated for no adjacent STs. Event 5 was a true spike event. It was rejected because the spike in T4 was too small to be detected. And the ST b appeared 80 ms after event 4, so that it was grouped as a new event. Except for spike b, the other AV spikes were detected and grouped properly. Fig. 3.5 (b)-(d) also shows that no ST events were detected from typical artifacts.

3.3.2 BP montage

The results of BP montage detection for ST events 9 and 10 in Fig. 3.5 (a) are shown in Fig. 3.6. As shown in Fig. 3.6 (a), even small BP spikes were detected. By single channel visual inspection, they might be identified as background activities, such as T3-T5 and T5-P3 in event 9. They might not be important for single channel detection, but they were meaningful to show the focus characteristic of spike activities. Without the BP ST in T5-P3, there were no connections to ST electrodes from P3, thus event 9 would be identified as no focus. The distribution of normalized weights is shown in Fig. 3.6 (b). Only the weights of electrodes near focus are displayed. The electrodes have lower weights if they have longer distance from focus. From the weight distribution, the focus characteristic of spike activities could be clearly observed, and the focus channel could be easily identified.

The focus channel of event 9 was declared as F7-T3, event 10 as no focus. For the other ST events in Fig. 3.5 (a), the focus channels were identified as below: 1, T4-T6; 3, F8-T4; 4, no focus; 6, T4-Av. Event 4 was declared as no focus because it had two ST electrodes and $\max\{W_i\}$=189μV, which was not enough. However, the focus characteristic of event 4 was clear: all the NST electrodes were connected to an ST electrode.

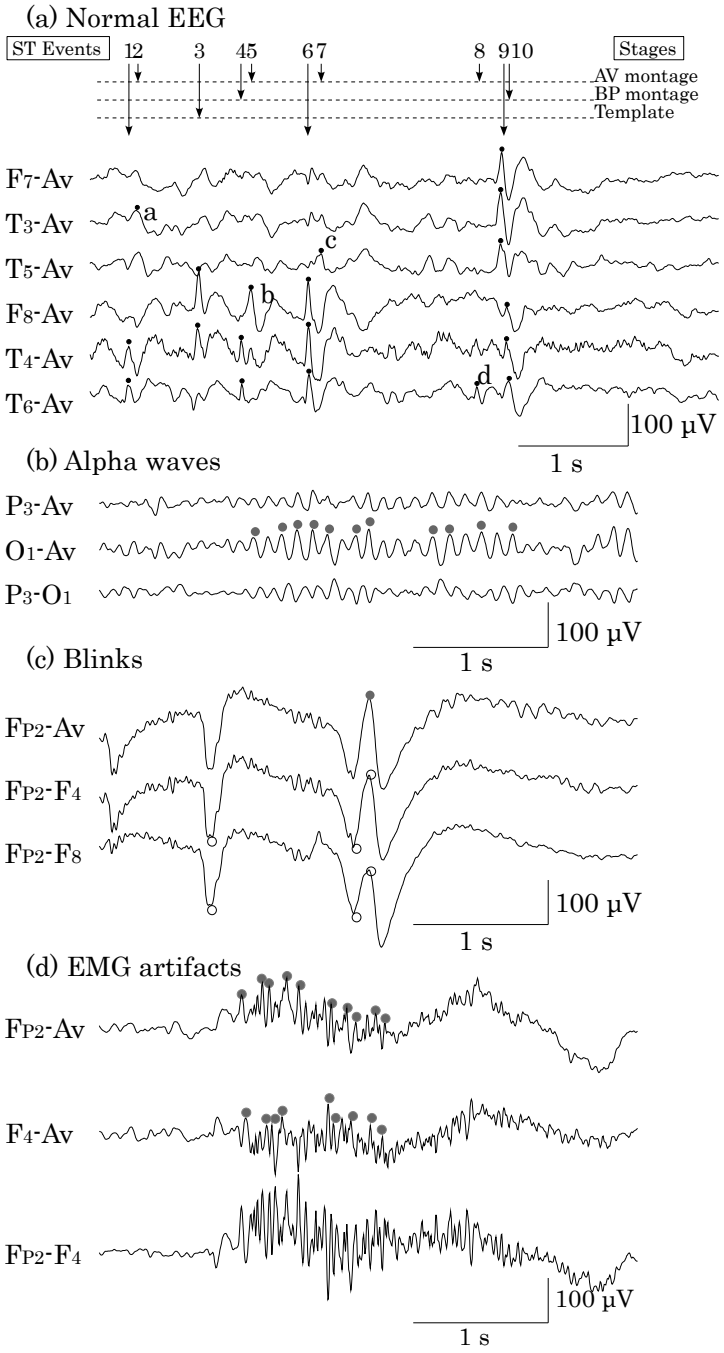

Fig. 3.5 Results of AV montage detection. (a) AV STs (black dots) and ST events (arrows) in normal EEG. All spikes were detected. (b) AV STs (gray dots) from alpha waves. All were rejected. In BP channel, alpha waves are attenuated. (c) One AV ST (the gray dot) was detected in *FP*2-*Av* and declared as a blink. If only detecting BP channels, all the peaks marked with circles will be detected. (d) AV STs (gray dots) from EMG artifacts. All were rejected. If only detecting *FP*2-*F*4, larger amplitude STs must be accounted.

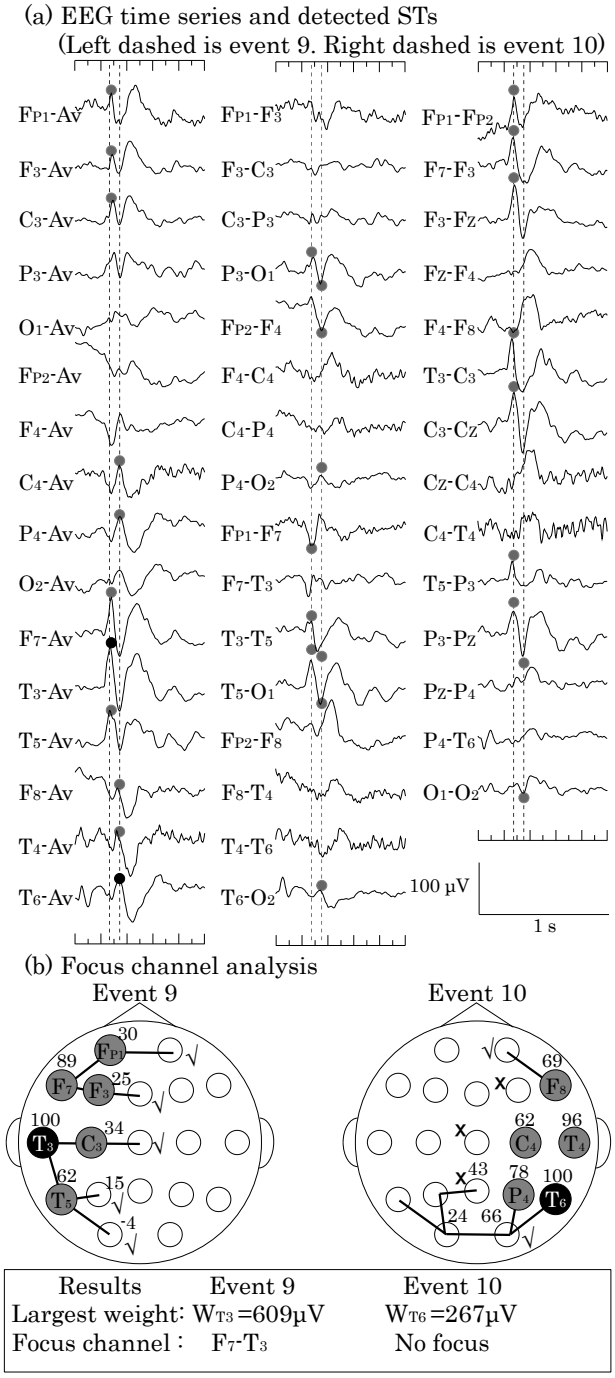

Fig. 3.6 Results of BP montage detection. (a) EEG time series of event 9 and 10 and detected STs. ST Events are marked with dashed. Black dots are focus AV STs. Gray dots are BP and adjacent AV STs. Small BP STs (e.g. T5-P3) were also detected. (b) Focus channel analysis. Black dots are focus ST electrodes. Gray dots are adjacent ST electrodes. BP STs are marked with lines. The NST electrodes marked with "√" and "×" are adjacent to ST electrodes. "√" indicates it is connected to an ST electrode by a BP ST. "×" indicates no BP STs between it and ST electrodes. The values beside electrodes are normalized weights ($100\times W_i=\max\{W_i\}$). From the distribution of weights, the focus channels were identified.

3.3.3 Multi-channel template

3.3.3.1 Event clustering

The clustering results of 6 recordings with spike activities are shown in Fig. 3.7. Effective focus channels are displayed as gray areas. Visual inspection proved that most ST events at ineffective focus channels were FPs.

3.3.3.2 Individual template

Four typical focus channels were selected from four patients. The distribution and overlapped waveforms of ST channels are shown in Fig. 3.8 (a)-(d). Clear focus characteristic were observed from the distribution. There were 6 ST channels for F8-T4 of S1, 9 for O2-Av of S2, 10 for F8-T4 of S4, and 16 for P3-Av of S6. The waveforms of positive BP ST channels were reversed for better inspection of similarity. S1 had highly correlated ST channels, as well as S4, and S6. S2 was an exception. The SW durations adaptable to individual patients are marked with dashed. S6 had a much shorter one than the others.

Fig. 3.8 shows significant differences between patients. S1 had clear spike and clear slow wave. S2 had various waveform patterns. Even for spike part, the largest duration was almost twice as longer as the least. For S4, the amplitude of slow wave was small but clear. In the case of S6, only 11 events were clustered at *P*3-*Av*, thus the waveforms were not smooth enough. However, the characteristics were obvious: clear and sharp spike part, clear slow wave, and highly correlated ST channels. Besides, 16 ST channels suggested spike activities could be observed in a larger area.

In order to study the correlation between patients, the AV channel with the largest *A*ST was selected for each: *T*4-*Av* for S1, *O*2-*Av* for S2, *T*4-*Av* for S4, and *P*3-*Av* for S6. They are shown with bold lines in Fig. 3.8 (a)-(d). The correlations are illustrated in Fig. 3.8 (e). Since SW durations were different, a fixed duration from -0.05 s to 0.5 s was used. Compared with visual inspection, the correlations reflected the similarities properly. The highest correlation of 0.92 was between S1 (*T*4- *Av*) and S6 (*P*3-*Av*), and the lowest of 0.18 appears between S2 (*O*2-*Av*) and S6 (*P*3-*Av*).

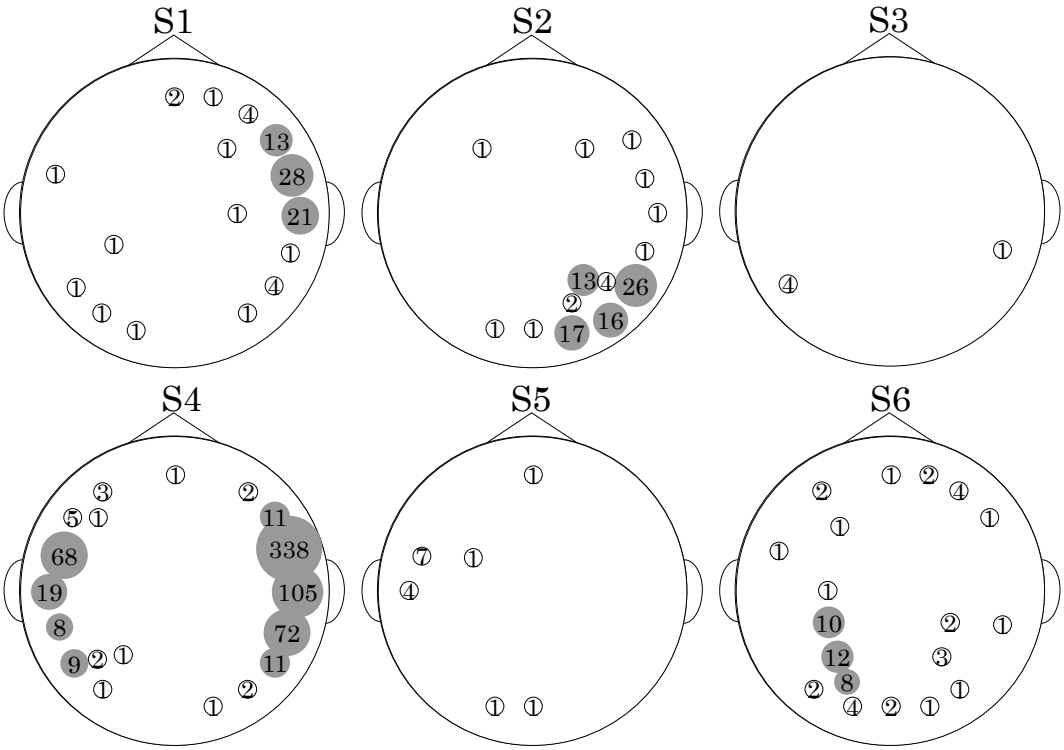

Fig. 3.7 Clustering results of the recordings with spike activities. The numbers are the amount of clustered ST events. Gray areas are effective focus channels, and circles are ineffective.

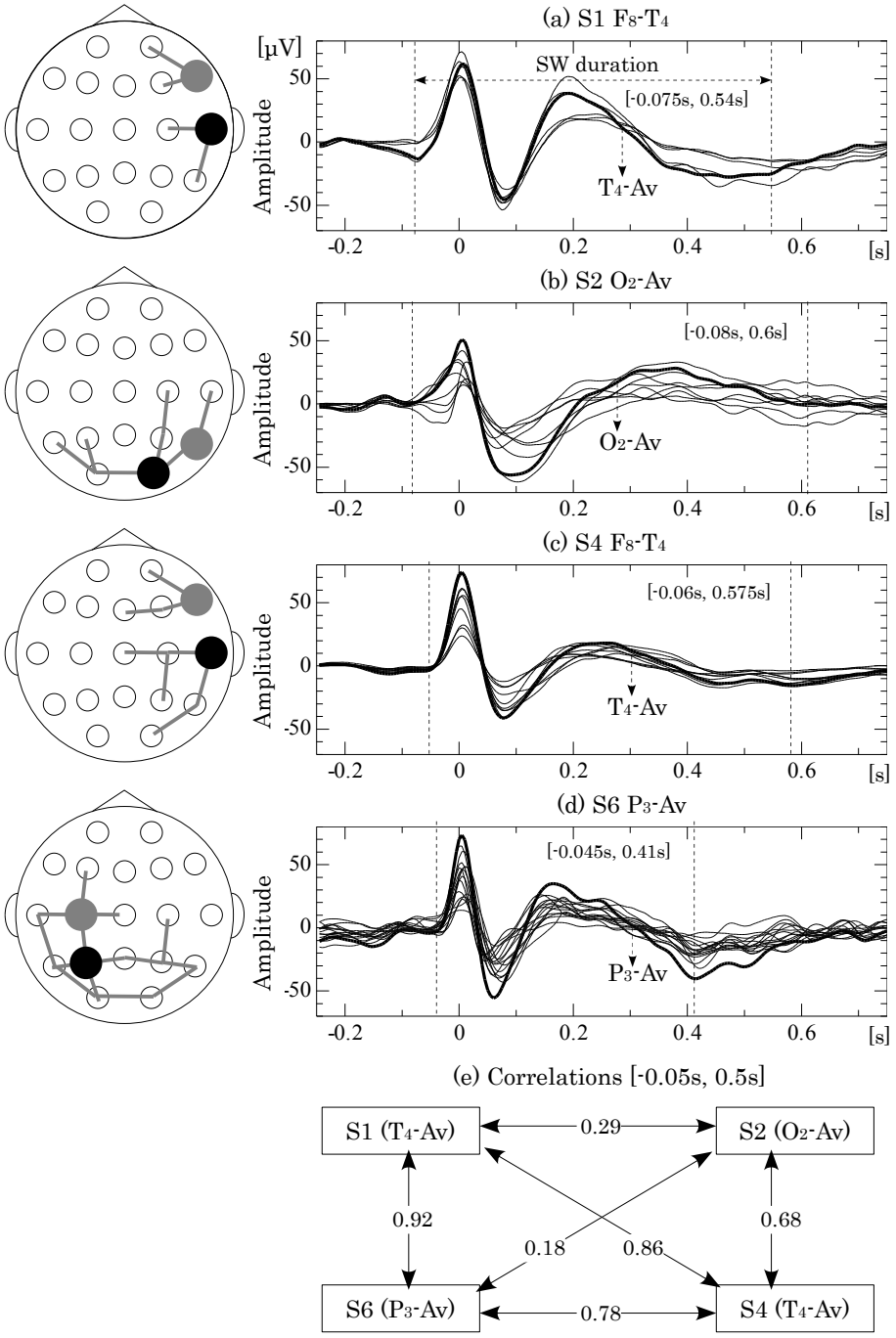

Fig. 3.8 ST channels of typical focus channels: (a) *F*8-*T*4 of S1, (b) *O*2-*Av* of S2, (c) *F*8-*T*4 of S4, (d) *P*3-*Av* of S6. Left is distribution. Dots and lines denote AV and BP channels. Right is overlapped waveforms. SW durations are marked with dashed. Positive BP ST channels are reversed for better visual inspection of similarity. (e) Correlations between typical AV channels (black dots and bold lines) with a fixed duration from -0.05 s to 0.5 s.

3.3.4 Performance

The spike detection system was programmed with C language and tested on a notebook. The required time depended on the recordings. For completing the analysis of S4, which included most spikes, about 70 seconds were required. Visual inspection of the results was done by an experienced expert, and the events difficult for judgment were selected and judged again by discussion of other three doctors. The results were assessed by selectivity, false positive rate per minute (FPM), sensitivity and specificity. The measures for calculation were defined in Table 3.3. We should note that the actual FN was less, because the events rejected by template matching included both spike and non-spike events. Therefore, the actual sensitivity was probably higher.

The results of all the 17 recordings are shown in Table 3.4. J1 was the results after BP montage stage. J2 was the results excluding ineffective focus channels. J3 was the TRUE events identified by template stage. For the records including spike activities (S1-S6), 11% events of J1 were rejected by clustering, and 30% of J2 were rejected by template method. The selectivity ranged from 92.6% (S6) to 97.0% (S4). The average FPM was 0.09. S4 had the highest FPM of 0.26. By visual inspection, 4 ST events in S3 and 7 in S5 were possible true spikes. They were rejected because the focus channels were declared as ineffective for inadequate ST events. S3 had one focus channel clustered 4 events; S5 had 6 focus channels (the most one clusters 7 events). For the records without spike activities (NS), 119 events were detected in all the 11 records. Since no effective focus channels were identified, all of them were rejected.

Table 3.3 Definition of measures

L	Length	The length of the recording in minutes
TE	Total events	$L \times N$. N* is the events in one minute
TP	True positive	True spike events after template stage
FP	False positive	Non-spike events after template stage
FN	False negative	The events rejected by template matching
TN**	True negative	The events rejected before template stage
Sel	Selectivity	TP/(TP+FP) ×100%
FPM	False positive rate per minute	FP/L
Sen	Sensitivity	TP/(TP+FN) ×100%
Spe	Specificity	TN/(TN+FP) ×100%

* N is defined as 120, i.e. one event for 0.5 s.

** TN is derived by TE-TP-FP-FN.

Table 3.4 Performance of the spike detection system

No	L [min]	J1	J2	J3 TP|FP	Sel [%]	FPM [/min]	Sen [%]	Spe [%]
S1	23	81	62	44|3	93.6	0.13	74.6	99.89
S2	46	86	72	52|4	92.9	0.09	76.5	99.93
S3	55	4	0	0|0	---	0	---	100
S4	50	659	640	421|13	97.0	0.26	67.1	99.76
S5	51	15	0	0|0	---	0	---	100
S5	8	59	30	25|2	92.6	0.25	89.3	99.79
Sum	233	904	804	542|22	96.1	0.09	69.3	99.92
NS	245	119	0	0|0	---	0	---	100

J1: After BP montage J2: After clustering J3: TRUE events
S1-S6: recordings including spike activities.
NS: 11 recordings without spike activities.
FN=J2-J3, TN=TE-TP-FP-FN=120×L-J2.

3.4 Discussion

3.4.1 Typical artifacts

The characteristics of typical artifacts were emphasized when we identified FPs in AV montage stage. Although the algorithms are not perfect, the most important characteristics have been considered. We have to pay attention to the following points when the algorithms are used.

Only the most typical alpha waves were directly eliminated. If the alpha waves in other channels were grouped as a event, the event would be identified as no focus in BP montage stage. Similarly, current conditions could only reject common blinks. The blinks with drift baseline or of small amplitude would not be declared. In this case, the focus channel was possibly identified at frontal area, and the event would be rejected for ineffective focus channel. If there were true spikes at frontal area, the events from blinks would be rejected by template matching. In the case of EMG artifacts, it was observed that some FPs from short time EMG artifacts (<0.5 s) were kept until clustering. Although it is difficult to identify them due to clear background activities, they could be finally eliminated in the template stage. As for slow waves, since almost all valuable negative peaks were checked, it was necessary to identify the obvious FPs from slow waves. If thresholds for sharpness were used, there was no need to consider slow waves. Finally, for identifying complex channels, the condition was rough but strict. However, the segments including continuous high amplitude

spikes could also be identified, since the power of theta and alpha waves were increased significantly. In this case, only high amplitude spikes would be kept.

3.4.2 Focus channel analysis

The focus characteristic has not been addressed sufficiently in published papers. Usually, the phase reversal of two channels is used. That is not enough for identification. We proposed a weighting method using the information of all BP STs to identify the focus channel of a event with a resolution of 16 AV channels and 30 BP channels. It is not only helpful to evaluate the focus location, but also effective to identify FPs beyond typical artifacts. As shown in Fig. 3.6, event 10 is caused by the AV reference. Comparing the focus ST channels of event 9 (*T*3-*Av*) and 10 (*T*6-*Av*), we can find that the half-waves of *N*1*P*2 in *T*3-*Av* and *P*1*N*1 in *T*6-*Av* are synchronous, and after subtraction in BP channels, sharp waves can not be observed in event 10. Moreover, the weighting method is also helpful to identify effective focus channels. As shown in Fig. 3.7, we only need to concentrate on the ST events at gray areas.

However, only the focus channel is not enough to present the characteristics of spike activities accurately. More measures should be taken into consideration. It is observed that even for the same focus channel, the distribution of BP STs may be different.

3.3.3 Multi-channel template

Although template method is well known as a typical spike detection method, it is seldom employed because of large individual difference and various patterns. In this chapter, template method is employed for spike confirmation rather than detection. Multi-channel, multi-montage templates for multi-focus with adaptable duration are extracted. Our results suggested that the template method is useful for both confirmation of spikes and rejection of FPs. As shown in Fig. 3.8 (b), the differences between channels are obvious. In this case, single channel template is not efficient. Besides, comparing the waveforms in Fig. 3.8 (a)-(d), we can also conclude that the adaptable duration including slow-waves is important to characterize spike activities.

However, current rules are not mature. Not all the spike activities can be confirmed. In the case of continuous spikes, the waveforms may be distorted and rejected. As shown in Fig. 3.5 (a), events 3, 4 and 5 are true spike events but rejected. The slow-wave of event 3 becomes shorter, and the AV ST in event 4 at *T*4-*Av* has two small spikes. Event 4 and 5 might originate from the same spike activity.

3.3.4 Comparison with other algorithms

Most papers identify the spike events and FPs by the same criteria using advanced algorithms [54,55,63,68,69,71,77,79-81,92-95,100,108,110,121,122]. They attempt to extract the characteristics of spikes accurately. On one hand, if we only focus on the characteristics of spike activities, it is difficult to identify all FPs without rejection of any true spikes. On the other hand, clinicians are not confident in advanced algorithms, because of invisible judgment procedure. Traditional advanced algorithms cannot provide clear reason of false judgment when detecting FNs or FPs. However, our algorithm employs the characteristics of FPs directly, so that it is easy to identify most typical FPs without rejection of true spike events. The algorithm can also give a clear reason if a false judgment is found, then the algorithm can be improved conveniently.

Hoef et al. studied nine patients using Stellate Harmonie System (Montreal, Canada) with different sets of spike detector settings [48]. The mean sensitivities for different detector settings were from 0.09 to 0.34, and the mean rates of FPs from 4.2 to 48.6 per hour. Some well-visualized EEG spikes that were not detected, were given as examples. From the examples, we assume the reason is waveform decomposition. Although waveform decomposition is the first step of most mimetic algorithms [29], it loses most information of morphology, so that even experts may have no confidence to identify spike activities correctly. Moreover, it is hard to judge the polarity of BP spikes by decomposed waveforms.

Glover et al. used a series of rules for elimination of FPs by context signals including electrocardiogram (ECG), EMG, and electrooculogram (EOG) [51], [52]. The system detected 95.7% (ranged from 80% to 100%) of the epileptiform events with a false detection rate of 11.1% (ranged from 5.3% to 35%) [52]. However, their method only detected spike part. Our method eliminates FPs only by EEG signals, and slow waves are also detected. Gotman and Wang proposed a state dependent method to reject artifacts [36]. Since mis-identification of state results in incorrect identification of FP, in our method, FPs are eliminated without considering states.

Nonclercq et al. proposed a single channel template method in [91]. Template method was employed twice with a fixed duration of 300 ms. The patient-specific template was extracted from the detections by original template made by generic parameters. However, using a template with fixed duration or focusing mainly on the spike may not be accurate enough. We use a multi-channel template method with adaptable durations considering slow wave. In other words, spatial template matching is used in our system and temporal template matching is proposed in [91].

3.3.5 Future work

However, the current method has its limitations in several aspects. First of all, it cannot be used for real-time analysis, since the template stage was from the viewpoint of whole records. For real-time analysis, template stage must be improved as time-varying. Second, our method is not designed for detecting whole night sleep EEG or ictal EEG. It is proposed as part of AEI system for routine EEG. All the 17 recordings tested in this chapter are awake EEG records. Third, since our method is developed on the basis of expert experience, only the 17 recordings are not enough to validate the effectiveness of the system. The system needs to be improved by new expert experience from new recordings. Besides, in order to reduce candidates from EMG artifacts, and precisely detect the key peaks of spikes, a digital band pass filter of 0.53-20 Hz was used. However, 20 Hz is not adequate to present the characteristics of spikes. We are developing the algorithms for EMG artifacts rejection and key peaks detection in the waveforms filtered by 60 Hz, which is a commonly used frequency.

3.5 Conclusions

In this chapter, we designed a multi-stage automatic EEG spike detection system. The results suggested that AV montage was efficient for candidate events selection, BP montage was accurate for focus identification, and the multi-channel template was effective to present the feature of frequent spikes. In the methods, the characteristics of typical FPs and the focus of spike activities were emphasized. Especially, a weighting method was established for focus analysis. For other systems, the proposed FPs detection algorithms could be a helpful complement.

Chapter 4

Automatic spike detection based on real-time multi-channel template

4.1 Introduction

Automatic spike detection is important for clinical diagnosis of epilepsy. In the past 30 years, a lot of research groups attempted kinds of methods. Most of these methods were purposed for off-line analysis. Some papers reported real-time application for seizure detection, but few for spike detection [44,62,126,127]. However, real-time application for spike detection has special meanings in clinical diagnosis. First, it can be used for real-time monitoring. It allows doctors to observe the symptom of patient during seizure. Second, it can be used for real-time reviewing. It allows doctors to end the recording when the disorder is determined. That will short the recording time and reduce the burden of patients. If a 2-hour record is enough for judgment, it is not necessary to record 4 hours.

Template method may be the best choice for real-time detection. But it was seldom used for the difficulty of preparing proper templates for all patients. Recently, Nonclercq et al. employed a single channel template method adapted to individual patients [91]. Ideal templates are adaptable to individual patient. Since the waveform patterns vary largely between individual patients, the template extracted from an patient should not be expected to used for another. The best template for each patient should be extracted from their own recordings. Even for one patient, the distribution of spike activities may be different from one event to another. Since single channel template is not enough to represent the differences, template method should be of multi-channel. There is no standard about how to classify spike events according to their distribution. Distribution is an intuitive concept. The most important characteristic is the focus position. We attempt to consider the focus channel as the basis of classifying spike events. The focus channel was evaluated accurately, then the template waveforms can be obtained properly. We found that template method has satisfactory performance.

The authors had developed a spike detection system for off-line analysis [128], [129]. The algorithm used large area spatial and temporal information. To some degree, it was like human from the viewpoint of judgment. Multi-channel template method was purposed in the paper. The classification with focus analysis is not perfect, and the rules for multi-channel template matching are simple, but the results are encouraging. This study developed the system for real-time application. The aim was no false positives (FPs) for the subjects without epilepsy. Real-time spikes can be detected with a delay of about 2 s.

4.2 Methods

4.2.1 Subjects and data acquisition

EEG signals had been recorded by a digital electroencephalograph (Nihon-Koden EEG2100) in the Kyoto University Hospital. Twenty-one electrodes including ear-lobes were placed according to the international 10-20 system. The EEG signals were recorded with a sampling frequency of 200 Hz and band-pass filtered by 0.016-120 Hz using hardware. The electrodes were referenced to a common referential electrode. The signals could be reformatted as any montages later. For simulation of real-time application, the digital electroencephalograph sent EEG to a DA board, and another computer for real-time detection received the EEG signals from the DA board via an AD board. The signals were updated every 0.32 s. Because of the limitation of AD and DA device, only 16- channel signals were available. In practice, if the detecting PC can receive the signals the same to EEG machine, 19-channel signals are preferred.

4.2.2 Off-line spike detection system

We had developed a system based on elimination of false positives for off-line EEG spike detection. Both common average reference (AV) montage and bipolar (BP) montage are considered. The block diagram of the three-stage system is shown in Fig. 4.1. The block diagram has been explained in detail in Section 3.2.

- **The AV montage stage** created candidate spike events by detecting AV channels. All the transients which were possible to be spikes were picked out. Artifacts were examined for each transient. Then the remained transients were grouped as events by spatial and temporal relations.
- **The BP montage stage** analyzed the focus channel of each event. Possible BP spikes were detected by a template method with adaptable durations. The focus

channel was identified by a weighting method integrating the information (polarity, amplitude and distribution) of all BP spikes.

- **The template stage** declared true spike events from a viewpoint of the whole recording. Events were clustered by focus channels. The multi-channel template was extracted only for the focus channels with sufficient events. Finally, a set of simple rules were used for template matching.

Elimination of FPs was carried out in all the stages. In the AV montage stage, typical artifacts and the events with single AV sharp transient were removed. In the BP montage stage, the events without focus were deleted. In the template stage, the events with ineffective focus channels were ignored.

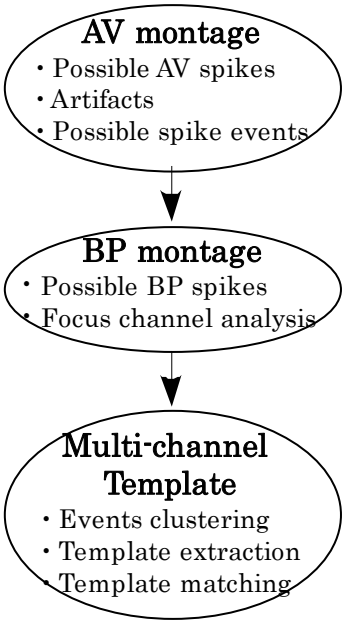

Fig. 4.1 Block diagram of off-line spike detection system. The AV montage stage created possible spike events. The BP montage stage emphasizes focus analysis. The template stage surveys the results from a viewpoint of the whole recording. False positive detection is carried out in all stages.

4.2.3 Real-time spike detection system

Except for ear-lobes, 16 AV channels were derived. Each electrode was referenced to the average potential of all 16 electrodes. Then 30 BP channels were derived from 16 AV channels. The AV channels of *FZ*, *CZ* and *PZ* are evaluated by the average of *F*3 and *F*4, *C*3 and *C*4, *P*3 and *P*4 respectively.

The records were detected three times for three stages in offline system. For real-time application, we must carry out the three stages simultaneously. Once AV montage stage detected a new candidate event, BP montage stage will analyze if the event has an effective focus channel. Similarly, If an event with effective focus

channel is identified by BP montage stage, template stage will match the event with the template of its focus channel:

- If the template is ineffective, the event will be declared as possible events, and used to update the template;
- If the template is effective, the event will be matched with existed template. If the event has high correlation with the template, the event is declared as definite spike events and used to update current template. Otherwise, the event will be declared as possible events, and the template is not changed.

The flowchart of real-time spike detection system is illustrated in Fig. 4.2. The three stages in off-line system are employed. After AV montage stage, all events are saved for further detection. After BP montage stage, the events with effective focus channels are saved as possible spike events. In template stage, multi-channel template are extracted from possible spike events, and the events passed template matching are declared as TRUE, i. e. definite spike events. There rules were used for template matching:

- The average correlation was larger than 0.4;
- The maximum correlation was larger than 0.77;
- There were at least three correlations larger than 0.7.

We should pay attention to two points for real-time application. First, in order to analyze background EEG activities, as shown in Fig. 4.3, the signals including 2-s before and after the detection sample is necessary. That results a time delay of 2-s, since the newest 2-s samples cannot be detected at once. Second, the real-time multi-channel template is extracted according to the following rules. For each focus channel:

- If there are less than 8 events, the template is extracted by averaging all the events, and declared as ineffective;
- Otherwise, the template is declared as effective, and only the TRUE events can update current template;
- TRUE events are defined as the events satisfying the rules for multi-channel template matching.

4.2.4 Monitor interface

The interface of monitor should consist of the following information or functions: a) EEG waveforms, can be switched between AV montage and two BP montages; b) spike events review; c) history trends of detection. Clinicians could stop the recording when adequate spikes are detected. Spike events could be identified with two levels of possible and definite. The possible ones should show clear focus characteristic. The definite ones should also show ideal waveform patterns.

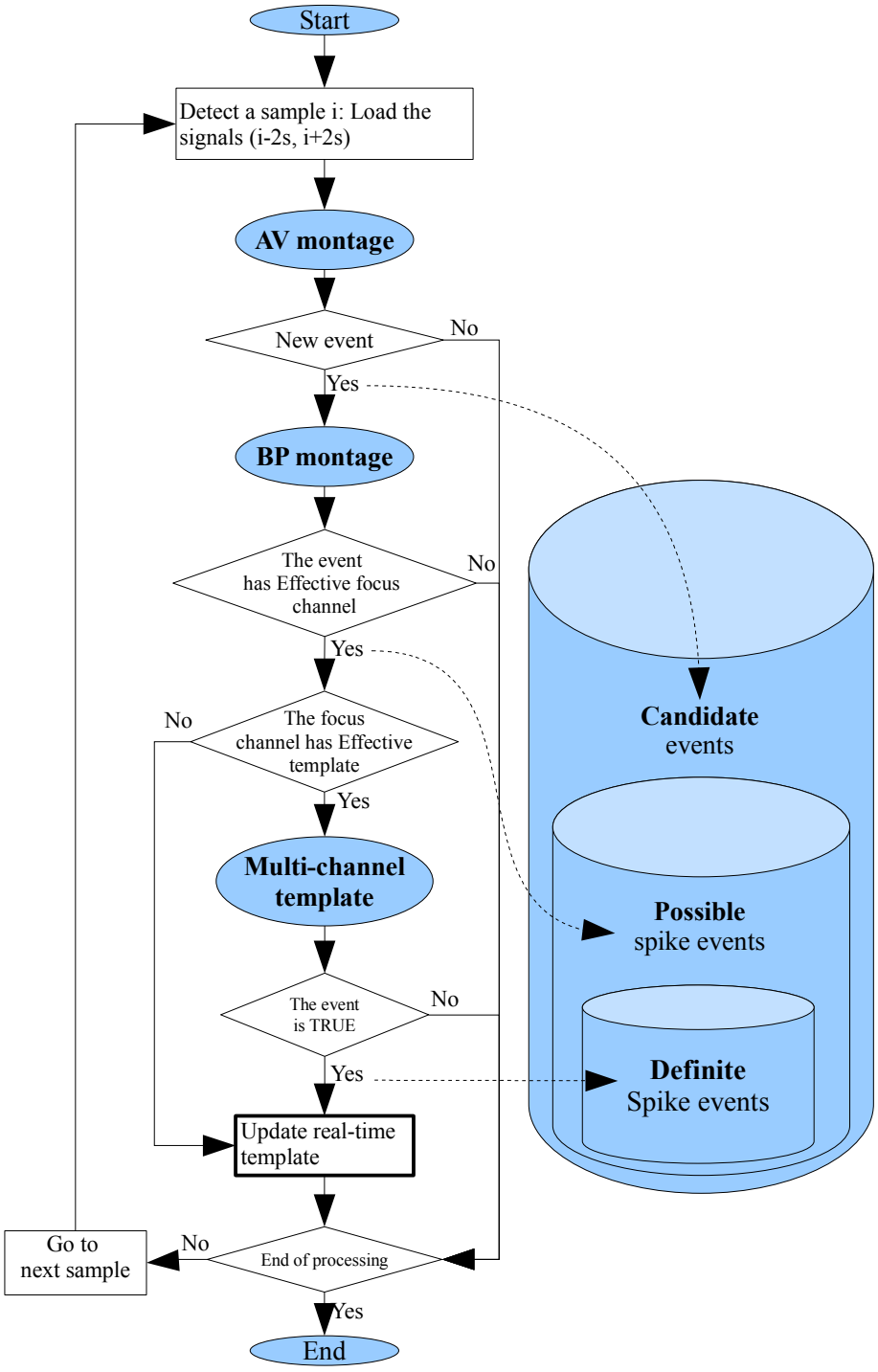

Fig. 4.2 The flowchart of real-time spike detection system. All the events with effective focus channels are defined as possible spike events. The events satisfying the rules for multi-channel template matching are declared as TRUE, and defined as definite spike events.

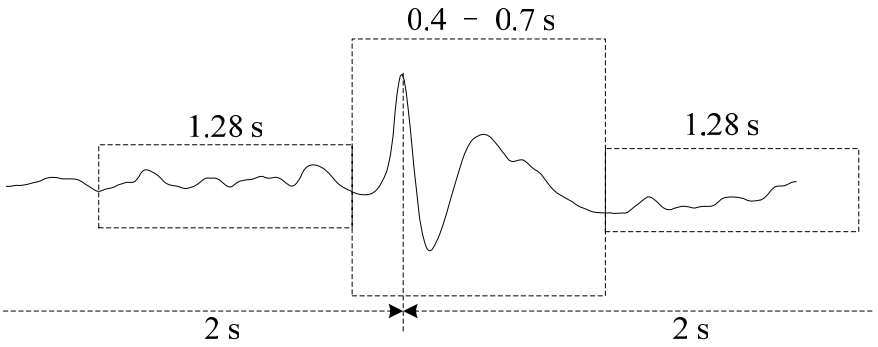

Fig. 4.3 The necessary duration. For analyzing background EEG activities, 2 s before and after the detecting sample is needed. The duration of spike activity including slow wave is usually from 0.4-0.7 s. Since the spike activities influence the spectral power significantly, the durations before spike part and after slow wave part is preferred.

4.3 Results

4.3.1 Real-time multi-channel template

The templates of two focus channels from one epilepsy patient are shown in Fig. 4.4. Only the channels at the right hemisphere are selected. The overlapped waveforms displayed three real-time templates, averaged from 8, 16, 24 events respectively. (1) For this patient, 8 events are enough for template extraction. (2) The slow waves of T4-Av are a little different in the two template. (3) The distribution of two templates are different. For example, considering AV channels, in Fig. 4 (a), clear spike waveforms are observed in F8-Av, T4- Av, T6-Av and C4-Av. In Fig. 4 (b), clear spike waveforms are observed only in F8-Av and T4-Av with higher amplitude. As for the channels not related to spike activities, they became flat after averaging. In Fig. 4, the overlapped waveforms suggested the three templates had high correlation with each other. In this example, the template from 8 events is effective enough. If too many false positives are included, the template may be not smooth and satisfactory. However, after waveform averaging, the influence of FPs is attenuated. Then, with template matching rules, the percentage of true spike events for template extraction could be increased.

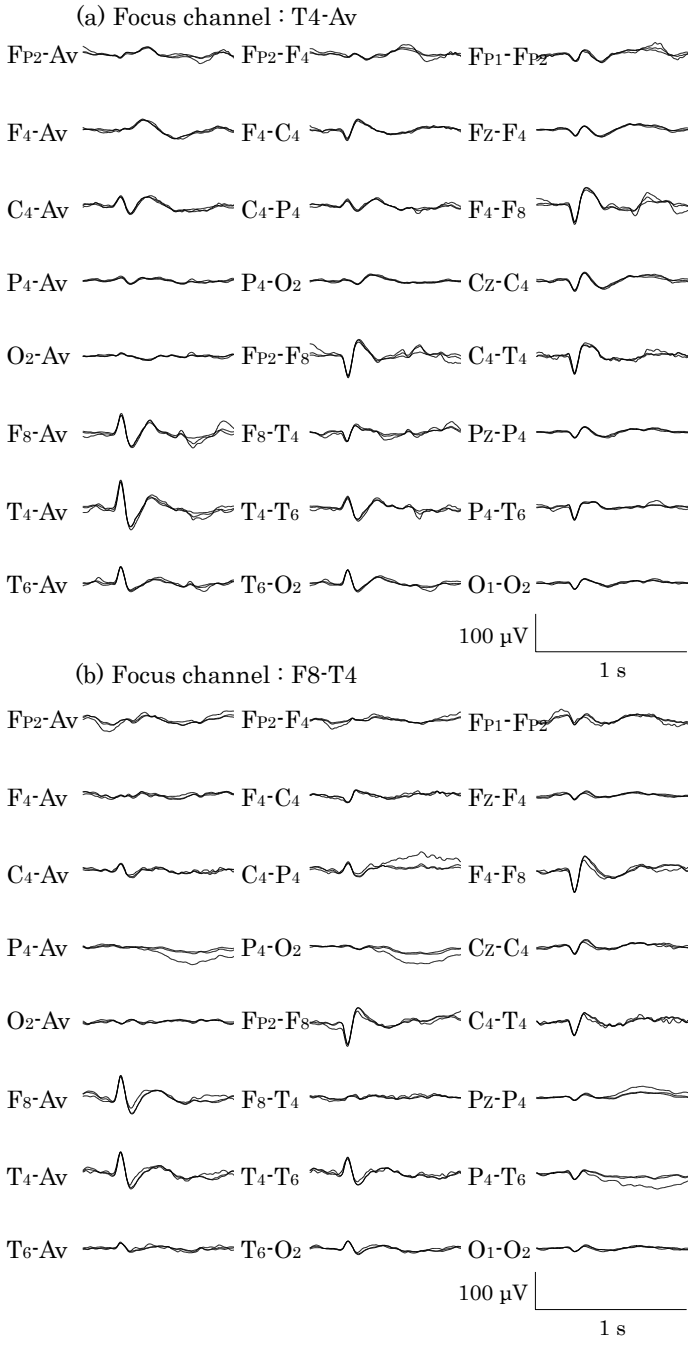

Fig. 4.4 The multi-channel templates of two focus channels from one patient. The overlapped waveforms illustrate three templates averaged from 8, 16 and 24 events respectively. (a) The template of T4-Av. (b) The template of F8-T4.

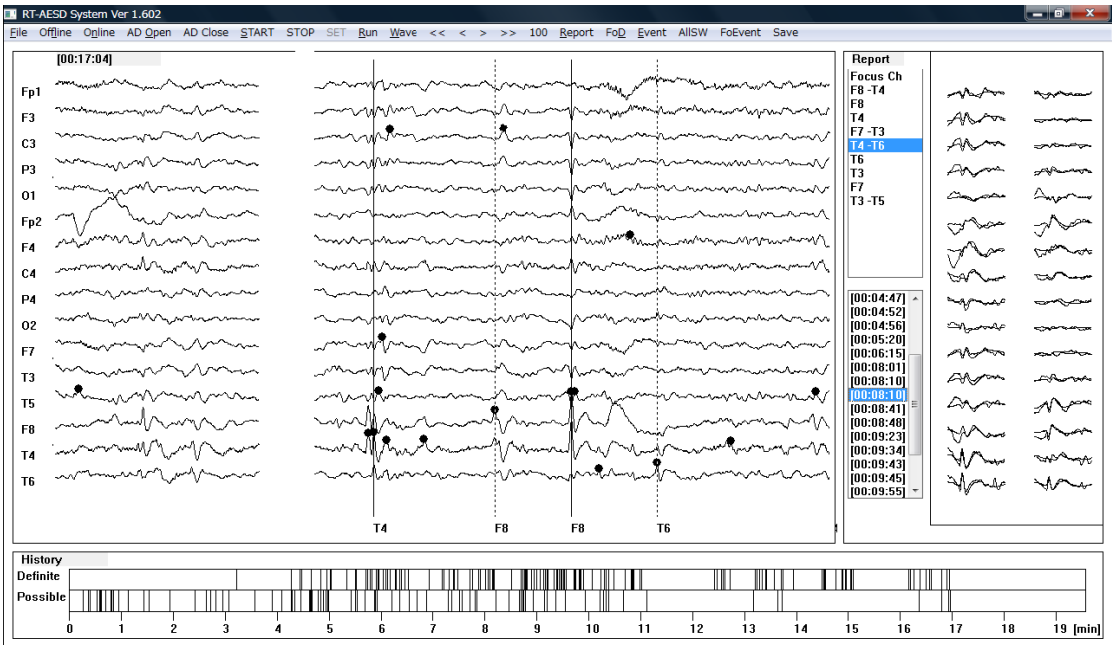

Fig. 4.5 Monitor interface. Part A displays the EEG waveforms, updating every 0.32 s. The dots indicate the AV channel of highest amplitude for all detected events. The dashed lines denote the events are identified as possible spike events. The solid lines denote the events are declared as TRUE, and identified as definite spike events. In Part B, the upper list box shows all detected focus channels. The lower list box shows all possible events for selected focus channel. The right of part B shows overlapped waveforms of selected events and the template of selected focus channel. 16 AV channels and 16 vertical BP channels are displayed. In part C, the history of detected possible and definite spike events are displayed.

4.3.2 Real-time system

The monitor interface is shown in Fig. 4.5, including three parts. Part A shows the EEG waveforms in real-time, updating every 0.32 s. All the events detected by AV montage stage are marked with dots at the AV channel of highest amplitude. All definite spike events are marked with solid lines. The possible spike events rejected by template stage are marked with dashed lines. In this example, 16 events are detected by AV montage stage, 4 events are declared as possible spike events by BP montage stage, 2 events are identified as definite spike events by template stage. The evaluation of these events is consistent with visual judgment. The definite events present better waveform patterns than the possible ones. Part B shows classified spike events. Two list boxes are shown at left. Detected focus channels are shown in the upper one and classified events of selected focus channel are shown in the lower one. At the right of part B, the overlapped waveforms of selected event and the template of its focus channel are displayed. It is easy to judge the similarities. Part C shows the

history trends of detection. The upper lines are definite spike events, and the lower lines are possible spike events. The distribution of spike activities on time scale is clear. Since no effective templates are declared during the first 3 minutes, no possible events are identified as definite. After 11 minutes, the templates of most focus channels are effective, so that more definite spike events are identified.

4.4 Discussion

4.4.1 Template method

Template method is a potential method for real-time spike detection, especially for the recordings of frequent spikes with stable morphology. Template method could tell doctors the common waveform patterns and the frequency of each pattern. Of course, because of distorted waveforms, true spikes may be missed and false positives may also be detected. However, the spike events highly related to the most typical waveform can be identified correctly. Template method can be combined with any other methods. Besides, template method should be used for spike confirmation rather than detection.

When using template method, the following items should be noted. **First**, the template should be of multi-channel. Single channel template is not enough to characterize the spike activities. **Second**, the distribution should be taken into account for classification. All the channels around focus are valuable for identification of spikes. Distribution is a very important information of individual patient. The difficulty is to extract characteristics for detection. In our method, we used the distribution to identify the focus channels. **Third**, before extracting template, the typical false positives should be removed. The effectiveness of templates is determined by the percentage of false positives. In other words, proper candidate events should be prepared by independent algorithms. As emphasized in Fig. 4.1, elimination of FPs is considered in all the stages. In this chapter, one recording with frequent spikes was tested. The results suggested that effective templates can be extracted from 8 events in the case of less false positives. **Four**, the rules for template matching should be considered carefully. Multi-channel template method used in this chapter is effective for real-time system, but not perfect. As shown in Fig. 4.4, the templates are good enough to identify spike events even only by template matching. The rules for multichannel template are still too simple. To establish proper rules for multi-channel template matching becomes a new problem. The rules should be considered in details. For example, high thresholds for spike part and lower thresholds for slow wave parts, because the slow waves are easier to be influenced by background activities.

4.4.2 Real-time system

We designed the real-time system considering the need of clinicians. The candidate events are identified with two levels of definite and possible. The ideal results are that all spike events are included with possible level, while all non-spike events are excluded with definite level. Since spike activities may be distorted especially for slow wave part, template method may reject true spike events. Even the events were rejected by template matching, they were still kept as possible spike events. For the recording with frequent spikes, only checking definite level events may be enough for diagnosis. But for the recording with occasional spikes, the possible level events are also valuable.

It should be noted that automatic detection is an assistant tool; the results must be identified by EEGers at last. False positives are serious, because normal people may be judged as patients if automatic systems are expected to be accurate and powerful. The emphasis of our system is to prove a given event to be non-spike activities. If we failed from all the view points, the event may be spike.

Chapter 5

Conclusions and future study

The analysis and interpretation of neuro-biological signals is an attractive topic. Doctors use neuro-biological signals by visual inspection to assist diagnosis of many disorders. In this thesis, automatic systems are developed for analysis of neuro-biological signals based on expert knowledge.

In **Chapter 1**, the background of the thesis is briefly discussed. The relationship between nervous system, brain and neuro-biological signals, EEG rhythms and recording, ECG and heart rate variability, the background of data classification and EEG spike detection, as well as the aim and structure of the thesis, are described.

In **Chapter 2**, a series of artifacts detection algorithms for real-time application was developed. Based on that, a real-time data classification model for accurate analysis of neuro-biological signals was proposed. As an example, a physical system to analyze the relationship between characteristics of EEG and ECG was developed. The results suggested that the proposed data classification method was effective. Comparing the best and worst segments, it was observed that contaminated signals would lead to mis-interpretation. With this system, it is convenient to monitor the quality of signals, acquire better understanding of artifacts, and obtain satisfactory recording.

Chapter 3 and **Chapter 4** are related to automatic EEG spike detection system for epilepsy diagnosis. The waveforms of spike activities vary greatly from one to another. Many methods have been attempted for automatic spike detection, but none of them are perfect because of large number of false detections. Most papers focused on identification of “spike activity”, while this system concentrated on identification of “non-spike activity”. In **Chapter 3**, a multi-stage automatic EEG spike detection system was designed. In this system, large area context was used. The results

suggested that AV montage was efficient for candidate events selection, BP montage was accurate for focus identification, and the multi-channel template was effective to present the feature of frequent spikes. In the methods, the characteristics of typical false positives (FPs) and the focus of spike activities were emphasized. Especially, a weighting method was established for focus analysis. For other systems, the proposed FPs detection algorithms could be a helpful complement. In **Chapter 4**, a real-time spike detection system was developed based on multi-channel template. Template method has advantages for real-time spike detection. Multi-channel template takes account of the distribution of spike activities and the individual differences between patients. Adaptable duration considering slow-wave for correlation analysis is recommended.

In future, the following topics are valuable to be investigated. First, the artifacts detection algorithms used for neuro-biological data classification could be improved. Currently, the recordings are judged for every 5 seconds in real-time. In practice, it is better to detect different artifacts with adaptable duration. Besides, the accuracy of the system needs to be verified by more recordings. Second, the common characteristics of non-spike activities are very useful for spike detection. Since identification of non-spike activity can improve the performance of any spike detection algorithm, without decreasing the specificity. On the other hand, it is easier to identify non-spike activities, such as blinks, EMG activities, and alpha waves. Third, multi-channel template method is effective for real-time spike detection system. However, in order to fully utilize template method, the current simple rules have to be improved.

References

Chapter 1 Introduction

[1] G. H. Klem, H. O. Lders, H. H. Jasper, and C. Elger, "The ten-twenty electrode system of the international federation," *Electroencephalogr Clin Neurophysiol Suppl.*, vol. 52, pp. 3-6, 1999.

[2] M. Nuwer. Assessment of digital EEG, quantitative EEG, and EEG brain mapping: Report of the American Academy of Neurology and the American Clinical Neurophysiology Society. *Neurology*, vol. 49, no. 1, pp. 277-292, 1997.

[3] E. H. Hon and S. T. Lee. Electronic evaluation of the fetal heart rate. VIII. Patterns preceding fetal death, further observations. *Am J Obstet Gynecol.*, vol. 87, pp. 814-826, 1963.

[4] B. M. Sayers. Analysis of heart rate variability. *Ergonomics*, vol. 16, no. 1, pp. 17-32, 1973.

[5] S. Akselrod, D. Gordon, F. A. Ubel, D. C. Shannon, A. C. Berger, and R. J. Cohen. Power spectrum analysis of heart rate fluctuation: a quantitative probe of beat-to-beat cardiovascular control. *Science*, vol. 213, no. 4504, pp. 220-222, 1981.

[6] B. Pomeranz, R. J. Macaulay, M. A. Caudill, I. Kutz, D. Adam, D. Gordon, K. M. Kilborn, A. C. Barger, D. C. Shannon, and R. J. Cohen. Assessment of autonomic function in humans by heart rate spectral analysis. *Am J Physiol.*, vol. 248, 1 Pt 2, H 151-153, 1985.

[7] M. Malik, T. Farrell, T. Cripps, and A. J. Camm. Heart rate variability in relation to prognosis after myocardial infarction: selection of optimal processing techniques. *Eur Heart J.*, vol. 10, no. 12, pp. 1060-1074, 1989.

[8] M. L. Appel, R. D. Berger, J. P. Saul, J. M. Smith, R. J. Cohen. Beat to beat variability in cardiovascular variables: noise or music?, *Journal of the American College of Cardiology*, vol. 14, no. 5, pp. 1139-1148, 1989.

[9] M. Malik, A. J. Camm. Heart rate variability. *Clinical cardiology*, vol. 13, no. 8, pp. 570-576, 1990.

[10] A. Malliani, F. Lombardi, M. Pagani. Power spectrum analysis of heart rate variability: a tool to explore neural regulatory mechanisms. *British heart journal*, vol. 71, no. 1, pp. 1-2, 1994.

[11] Task Force of the European Society of Cardiology and the North American Society of Pacing and Electrophysiology, Heart rate variability: Standards of

measurement, physiological interpretation, and clinical use, *Eur Heart J.*, vol. 17, no. 3, pp.354-381, 1996.

[12] D. Sapoznikov, M. H. Luria, Y. Mahler, M. S. Gotsman. Computer processing of artifact and arrhythmias in heart rate variability analysis. *Computer methods and programs in biomedicine*, vol. 39, no. 1-2, pp. 75-84, 1992.

[13] G. G. Berntson, J. R. Stowell. ECG artifacts and heart period variability: don't miss a beat! *Psychophysiology*, vol. 35, no. 1, pp. 127-132, 1998.

[14] X. Xu, S. Schuckers, CHIME Study Group. Automatic detection of artifacts in heart period data. *Journal of electrocardiology*, vol. 34 Suppl, pp. 205-210, 2001.

[15] L. Pezard, R. Jech and E. Ruzicka, Investigation of non-linear properties of multichannel EEG in the early stages of Parkinson's disease, *Clin Neurophysiol.*, vol. 112, no. 1, pp.38-45, 2001.

[16] N. Mammone and F.C. Morabito, Enhanced automatic artifact detection based on independent component analysis and Renyi's entropy, *Neural Netw.*, vol. 21, no. 7, pp. 1029-1040, 2008.

[17] J. F. Gao, Y. Yang, P. Lin, P. Wang and C. X. Zheng, Automatic removal of eye-movement and blink artifacts from EEG signals, *Brain Topogr.*, vol. 23, no. 1, pp.105-114, 2010.

[18] P. LeVan, E. Urrestarazu and J. Gotman, A system for automatic artifact removal in ictal scalp EEG based on independent component analysis and Bayesian classification, *Clin Neurophysiol.*, vol. 117, no. 4, pp. 912-927, 2006.

[19] A. Delorme, T. Sejnowski and S. Makeig, Enhanced detection of artifacts in EEG data using higher-order statistics and independent component analysis, *Neuroimage*, vol. 34, no. 4, pp. 1443-1449, 2007.

[20] J. A. Jiang, C. F. Chao, M. J. Chiu, R.G. Lee, C. L. Tseng and R. Lin, An automatic analysis method for detecting and eliminating ECG artifacts in EEG, *Comput Biol Med.*, vol. 37, no. 11, pp. 1660-1671, 2007.

[21] M. van de Velde, I. R. Ghosh and P. J. Cluitmans, Context related artefact detection in prolonged EEG recordings, *Comput Methods Programs Biomed.*, vol. 60, no. 3, pp. 183-196, 1999.

[22] R. Agarwal, J. Gotman, D. Flanagan and B. Rosenblatt, Automatic EEG analysis during long-term monitoring in the ICU, *Electroencephalogr Clin Neurophysiol.*, vol. 107, no. 1, pp. 44-58, 1998.

[23] P. J. Durka, H. Klekowicz, K. J. Blinowska, W. Szelenberger and S. Niemcewicz, A simple system for detection of EEG artifacts in polysomnographic recordings, *IEEE Trans Biomed Eng.*, vol. 50, no. 4, pp. 526-528, 2003.

[24] G. E. Chatrian, L. Bergamini, M. Dondey, D. W. Klass, M. Lennox-Buchthal, I. Petersén. A glossary of terms most commonly used by clinical electroencephalographers. *Electroencephalography and clinical neurophysiology*, vol. 37, no. 5, pp. 538-548, 1974.

[25] J. D. Jr Frost, Automatic recognition and characterization of epileptiform

discharges in the human EEG. *J Clin Neurophysiol.*, vol. 2, no. 3, pp. 231-249, 1985.

[26] J. Gotman. Practical use of computer-assisted EEG interpretation in epilepsy. *Journal of clinical neurophysiology*, vol. 2, no. 3, pp. 251-265, 1985.

[27] J. R. Hughes. The significance of the interictal spike discharge: a review. *J Clin Neurophysiol.*, vol. 6, no. 3, pp. 207-226, 1989.

[28] J. Gotman. Automatic detection of seizures and spikes. *J Clin Neurophysiol.*, vol. 16, no. 2, pp. 130-140, 1999.

[29] S. B. Wilson and R. Emerson. Spike detection: a review and comparison of algorithms. *Clin Neurophysiol.*, Vol. 113, No. 12, pp. 1873-1881, 2002.

[30] Harner R. Automatic EEG spike detection. *Clin EEG Neurosci.*, vol. 40, no. 4, pp. 262-270, 2009.

[31] E. Rodin, T. Constantino, S. Rampp, P. K. Wong. Spikes and epilepsy. *Clin EEG Neurosci.*, vol. 40, no. 4, pp. 288-299, 2009.

[32] J. J. Halford. Computerized epileptiform transient detection in the scalp electroencephalogram: obstacles to progress and the example of computerized ECG interpretation. *Clin Neurophysiol.*, vol. 120, no. 11, pp. 1909-1915, 2009.

[33] J. Gotman and P. Gloor. Automatic recognition and quantification of interictal epileptic activity in the human scalp EEG. *Electroencephalography and clinical neurophysiology*, vol. 41, no. 5, pp. 513-529, 1976.

[34] J. Gotman, J. R. Ives, and P. Gloor. Automatic recognition of inter-ictal epileptic activity in prolonged EEG recordings. *Electroencephalography and clinical neurophysiology*, vol. 46, no. 5, pp. 510-520, 1979.

[35] J. Gotman. Automatic recognition of epileptic seizures in the EEG. *Electroencephalography and clinical neurophysiology*, vol. 54, no. 5, pp. 530-540, 1982.

[36] J. Gotman and L. Y. Wang. State-dependent spike detection: concepts and preliminary results. *Electroencephalography and clinical neurophysiology*, vol. 79, no. 1, pp. 11-19, 1991.

[37] J. Gotman and L. Y. Wang. State dependent spike detection: validation. *Electroencephalography and clinical neurophysiology*, vol. 83, no. 1, pp. 12-18, 1992.

[38] J. Gotman, D. Flanagan, J. Zhang, and B. Rosenblatt. Automatic seizure detection in the newborn: methods and initial evaluation. *Electroencephalography and clinical neurophysiology*, vol. 103, no. 3, pp. 356-362, 1997.

[39] R. Agarwal, J. Gotman, D. Flanagan, and B. Rosenblatt. Automatic EEG analysis during long-term monitoring in the ICU. *Electroencephalography and clinical neurophysiology*, vol. 107, no. 1, pp. 44-58, 1998.

[40] K. Kobayashi, I. Merlet, and J. Gotman. Separation of spikes from background by independent component analysis with dipole modeling and comparison to intracranial recording. *Clinical neurophysiology*, vol. 112, no. 3, pp. 405-413, 2001.

[41] D. Flanagan, R. Agarwal, and J. Gotman. Computer-aided spatial classification of

epileptic spikes. *Journal of clinical neurophysiology*, vol. 19, no. 2, pp. 125-135, 2002.

[42] D. Flanagan, R. Agarwal, Y. H. Wang, and J. Gotman. Improvement in the performance of automated spike detection using dipole source features for artefact rejection. *Clinical neurophysiology*, vol. 114, no. 1, pp. 38-49, 2003.

[43] K. Kobayashi, H. Yoshinaga, M. Oka, Y. Ohtsuka, and J. Gotman. A simulation study of the error in dipole source localization for EEG spikes with a realistic head model. *Clinical neurophysiology*, vol. 114, no. 6, pp. 1069-1078, 2003.

[44] M. E. Saab and J. Gotman. A system to detect the onset of epileptic seizures in scalp EEG. *Clinical neurophysiology*, vol. 116, no. 2, pp. 427-442, 2005.

[45] K. Kobayashi, H. Yoshinaga, Y. Ohtsuka, and J. Gotman. Dipole modeling of epileptic spikes can be accurate or misleading. *Epilepsia*, vol. 46, no. 3, pp. 397-408, 2005.

[46] C. Grova, J. Daunizeau, J. M. Lina, C. G. Bénar, H. Benali, and J. Gotman. Evaluation of EEG localization methods using realistic simulations of interictal spikes. *NeuroImage*, vol. 29, no. 3, pp. 734-753, 2006.

[47] P. LeVan, E. Urrestarazu, and J. Gotman. A system for automatic artifact removal in ictal scalp EEG based on independent component analysis and Bayesian classification. *Clinical neurophysiology*, vol. 117, no. 4, pp. 912-927, 2006.

[48] L. Ver Hoef, R. Elgavish, and R. C. Knowlton. Effect of detection parameters on automated electroencephalography spike detection sensitivity and false-positive rate. *Journal of clinical neurophysiology*, vol. 27, no. 1, pp. 12-16, 2010.

[49] J. D. Frost, C. E. Hillman, P. Kellaway. Automatic interpretation of EEG: analysis of background activity. *Computers and biomedical research*, vol. 13, no. 3, pp. 242-257, 1980.

[50] P. Y. Ktonas, W. M. Luoh, M. L. Kejariwal, E. L. Reilly, and M. A. Seward. Computer-aided quantification of EEG spike and sharp wave characteristics. *Electroencephalography and clinical neurophysiology*, vol. 51, no. 3, pp. 237-243, 1981.

[51] J. R. Glover, N. Raghavan, P. Y. Ktonas, and J. D. Frost. Context-based automated detection of epileptogenic sharp transients in the EEG: elimination of false positives. *IEEE transactions on bio-medical engineering*, vol. 36, no. 5, pp. 519-527, 1989.

[52] B. Ramabhadran, J. D. Frost, J. R. Glover, and P. Y. Ktonas. An automated system for epileptogenic focus localization in the electroencephalogram. *Journal of clinical neurophysiology*, Vol. 16, No. 1, pp. 59-68, 1999.

[53] B. L. Davey, W. R. Fright, G. J. Carroll, and R. D. Jones. Expert system approach to detection of epileptiform activity in the EEG. *Medical & biological engineering & computing*, vol. 27, no. 4, pp. 365-370, 1989.

[54] A. A. Dingle, R. D. Jones, G. J. Carroll, and W. R. Fright. A multistage system to detect epileptiform activity in the EEG. *IEEE transactions on bio-medical*

engineering, vol. 40, no. 12, pp. 1260-1268, 1993.

[55] C. J. James, R. D. Jones, P. J. Bones, and G. J. Carroll. Detection of epileptiform discharges in the EEG by a hybrid system comprising mimetic, self-organized artificial neural network, and fuzzy logic stages. *Clinical neurophysiology*, vol. 110, no. 12, pp. 2049-2063, 1999.

[56] M. A. Black, R. D. Jones, G. J. Carroll, A. A. Dingle, I. M. Donaldson, and P. J. Parkin. Real-time detection of epileptiform activity in the EEG: a blinded clinical trial. *Clinical EEG*, vol. 31, no. 3, pp. 122-130, 2000.

[57] H. Goelz, R. D. Jones, and P. J. Bones. Wavelet analysis of transient biomedical signals and its application to detection of epileptiform activity in the EEG. *Clinical EEG*, vol. 31, no. 4, pp. 181-191, 2000.

[58] B. Vanrumste, R. D. Jones, P. J. Bones, and G. J. Carroll. Slow-wave activity arising from the same area as epileptiform activity in the EEG of paediatric patients with focal epilepsy. *Clinical neurophysiology*, vol. 116, no. 1, pp. 9-17, 2005.

[59] P. Van Hese, B. Vanrumste, H. Hallez, G. J. Carroll, K. Vonck, R. D. Jones, P. J. Bones, Y. D'Asseler, and I. Lemahieu. Detection of focal epileptiform events in the EEG by spatio-temporal dipole clustering. *Clinical neurophysiology*, vol. 119, no. 8, pp. 1756-1770, 2008.

[60] S. B. Wilson, R. N. Harner, F. H. Duffy, B. R. Tharp, M. R. Nuwer, and M. R. Sperling. Spike detection. I. Correlation and reliability of human experts. *Electroencephalography and clinical neurophysiology*, vol. 98, no. 3, pp. 186-198, 1996.

[61] S. B. Wilson, C. A. Turner, R. G. Emerson, and M. L. Scheuer. Spike detection II: automatic, perception-based detection and clustering. *Clinical neurophysiology*, vol. 110, no. 3, pp. 404-411, 1999.

[62] S. B. Wilson, M. L. Scheuer, R. G. Emerson, and A. J. Gabor. Seizure detection: evaluation of the Reveal algorithm. *Clinical neurophysiology*, Vol. 115, No. 10, pp. 2280-2291, 2004.

[63] A. J. Gabor and M. Seyal. Automated interictal EEG spike detection using artificial neural networks. *Electroencephalography and clinical neurophysiology*, vol. 83, no. 5, pp. 271-280, 1992.

[64] G. Jandó, R. M. Siegel, Z. Horváth, and G. Buzsáki. Pattern recognition of the electroencephalogram by artificial neural networks. *Electroencephalography and clinical neurophysiology*, vol. 86, no. 2, pp. 100-109, 1993.

[65] W. R. Webber, B. Litt, K. Wilson, and R. P. Lesser. Practical detection of epileptiform discharges (EDs) in the EEG using an artificial neural network: a comparison of raw and parameterized EEG data. *Electroencephalography and clinical neurophysiology*, vol. 91, no. 3, pp. 194-204, 1994.

[66] T. Kalayci and O. Ozdamar. Wavelet preprocessing for automated neural network detection of EEG spikes. *IEEE Engineering in Medicine and Biology Magazine*,

vol. 14, no. 2, pp. 160-166, 1995.

[67] O. Ozdamar and T. Kalayci. Detection of spikes with artificial neural networks using raw EEG. *Computers and biomedical research*, vol. 31, no. 2, pp. 122-142, 1998.

[68] C. W. Ko and H. W. Chung. Automatic spike detection via an artificial neural network using raw EEG data: effects of data preparation and implications in the limitations of online recognition. *Clinical neurophysiology*, vol. 111, no. 3, pp. 477-481, 2000.

[69] C. Kurth, F. Gilliam, and B. J. Steinhoff. EEG spike detection with a Kohonen feature map. *Annals of biomedical engineering*, vol. 28, no. 11, pp. 1362-1369, 2000.

[70] A. T. Tzallas, P. S. Karvelis, C. D. Katsis, D. I. Fotiadis, S. Giannopoulos, and S. Konitsiotis. A method for classification of transient events in EEG recordings: application to epilepsy diagnosis. *Methods of information in medicine*, vol. 45, no. 6, pp. 610-621, 2006.

[71] C. E. D'Attellis, S. I. Isaacson, and R. O. Sirne. Detection of epileptic events in electroencephalograms using wavelet analysis. *Annals of biomedical engineering*, vol. 25, no. 2, pp. 286-293, 1997.

[72] F. Sartoretto and M. Ermani. Automatic detection of epileptiform activity by single-level wavelet analysis. *Clinical neurophysiology*, vol. 110, no. 2, pp. 239-249, 1999.

[73] L. Senhadji and F. Wendling. Epileptic transient detection: wavelets and time-frequency approaches. *Neurophysiol Clin.*, vol. 32, no. 3, pp. 175-192, 2002.

[74] M. Latka, Z. Was, A. Kozik, B. J. West. Wavelet analysis of epileptic spikes. *Physical review. E, Statistical, nonlinear, and soft matter physics*, vol. 67, no. 5 Pt 1, 2003.

[75] H. Adeli, Z. Zhou, N. Dadmehr. Analysis of EEG records in an epileptic patient using wavelet transform. *Journal of neuroscience methods*, vol. 123, no. 1, pp. 69-87, 2003.

[76] Z. Nenadic and J. W. Burdick. Spike detection using the continuous wavelet transform. *IEEE transactions on bio-medical engineering*, vol. 52, no. 1, pp. 74-87, 2005.

[77] K. P. Indiradevi, Elizabeth Elias, P. S. Sathidevi, S. Dinesh Nayak, and K. Radhakrishnan. A multi-level wavelet approach for automatic detection of epileptic spikes in the electroencephalogram. *Computers in biology and medicine*, vol. 38, no. 7, pp. 805-816, 2008.

[78] H. S. Park, Y. H. Lee, N. G. Kim, D. S. Lee, and S. I. Kim. Detection of epileptic-form activities in the EEG using neural network and expert system. *Studies in health technology and informatics*, vol. 52 Pt 2, pp. 1255-1259, 1998.

[79] H. S. Liu, T. Zhang, and F. S. Yang. A multistage, multimethod approach for automatic detection and classification of epileptiform EEG. *IEEE transactions on*

bio-medical engineering, vol. 49, no. 12 Pt 2, pp. 1557-1566, 2002.

[80] N. Acir, I. Oztura, M. Kuntalp, B. Baklan, and C. Güzeliş. Automatic detection of epileptiform events in EEG by a three-stage procedure based on artificial neural networks. *IEEE transactions on bio-medical engineering*, vol. 52, no. 1, pp. 30-40, 2005.

[81] F. I. Argoud, F. M. De Azevedo, J. M. Neto, and E. Grillo. SADE3: an effective system for automated detection of epileptiform events in long-term EEG based on context information. *Medical & biological engineering & computing*, vol. 44, no. 6, pp. 459-470, 2006.

[82] J. R. Smith. Automatic analysis and detection of EEG spikes. *IEEE transactions on bio-medical engineering*, vol. 21, no. 1, pp. 1-7, 1974.

[83] J. F. Lemieux and W. T. Blume. Automated morphological analysis of spikes and sharp waves in human electrocorticograms. *Electroencephalography and clinical neurophysiology*, vol. 55, no. 1, pp. 45-50, 1983.

[84] J. C. Principe and J. R. Smith. Automatic recognition of spike and wave bursts. *Electroencephalography and clinical neurophysiology Suppl.*, vol. 37, pp. 115-132, 1985.

[85] T. Pietilä, S. Vapaakoski, U. Nousiainen, A. Värri, H. Frey, V. Häkkinen, and Y. Neuvo. Evaluation of a computerized system for recognition of epileptic activity during long-term EEG recording. *Electroencephalography and clinical neurophysiology*, vol. 90, no. 6, pp. 438-443, 1994.

[86] R. Benlamri. An automated system for analysis and interpretation of epileptiform activity in the EEG. *Computers in Biology and Medicine*, vol. 27, no. 2, pp. 129-139, 1997.

[87] T. Sugi, M. Nakamura, A. Ikeda, and H. Shibasaki. Adaptive EEG spike detection: determination of threshold values based on conditional probability. *Front Med Biol Eng.*, Vol. 11, No. 4, pp. 261-277, 2002.

[88] J. R. Stevens, B. L. Lonsbury and S. L. Goel. Seizure occurrence and interspike interval. Telemetered electroencephalogram studies. *Arch Neurol.*, Vol. 26, No. 5, pp. 409-419, 1972.

[89] R. Sankar and J. Natour. Automatic computer analysis of transients in EEG. *Computers in biology and medicine*, vol. 22, no. 6, pp. 407-422, 1992.

[90] S. Kim and J. Mcnames. Automatic spike detection based on adaptive template matching for extracellular neural recordings. Journal of Neuroscience Methods, vol. 165, no. 2, pp. 165-174, 2007.

[91] A. Nonclercq, M. Foulon, D. Verheulpen, C. De Cock, M. Buzatu, P. Mathys, and P. Van Bogaert. Spike detection algorithm automatically adapted to individual patients applied to spike-and-wave percentage quantification. *Neurophysiologie clinique*, vol. 39, no. 2, pp. 123-131, 2009.

[92] E. Urrestarazu, J. Iriarte, J. Artieda, M. Alegre, M. Valencia, and C. Viteri. Independent component analysis separates spikes of different origin in the EEG.

Journal of clinical neurophysiology, vol. 23, no. 1, pp. 72-78, 2006.

[93] M. De Lucia, J. Fritschy, P. Dayan, and D. S. Holder. A novel method for automated classification of epileptiform activity in the human electroencephalogram-based on independent component analysis. *Medical & biological engineering & computing*, vol. 46, no. 3, pp. 263-272, 2008.

[94] Tzallas AT, Oikonomou VP, Fotiadis DI. Epileptic spike detection using a Kalman filter based approach. *Conf Proc IEEE Eng Med Biol Soc*. vol. 1, pp. 501-504, 2006.

[95] V. P. Oikonomou, A. T. Tzallas, D. I. Fotiadis. A Kalman filter based methodology for EEG spike enhancement. *Computer methods and programs in biomedicine*, vol. 85, no. 2, pp. 101-108, 2007.

[96] M. Adjouadi, D. Sanchez, M. Cabrerizo, M. Ayala, P. Jayakar, I. Yaylali, and A. Barreto. Interictal Spike Detection Using the Walsh Transform. *IEEE Transactions on Biomedical Engineering*, vol. 51, no. 5, pp. 868-872, 2004.

[97] M. Adjouadi, M. Cabrerizo, M. Ayala, D. Sanchez, I. Yaylali, P. Jayakar, and A. Barreto. Detection of interictal spikes and artifactual data through orthogonal transformations. *Journal of clinical neurophysiology*, vol. 22, no. 1, pp. 53-64, 2005.

[98] S. Nishida, M. Nakamura, A. Ikeda, and H. Shibasaki. Signal separation of background EEG and spike by using morphological filter. *Medical engineering & physics*, Vol. 21, No. 9, pp. 601-608, 1999.

[99] W. Jia, R. J. Sclabassi, L. S. Pon, M. L. Scheuer, and M. Sun. Spike separation from EEG/MEG data using morphological filter and wavelet transform. *Conf Proc IEEE Eng Med Biol Soc*. vol. 1, pp. 6137-6140, 2006.

[100] G. H. Xu, J. Wang, Q. Zhang, S. C. Zhang, and J. M. Zhu. A spike detection method in EEG based on improved morphological filter. *Computers in biology and medicine*, Vol. 37, No. 11, pp. 1647-1652, 2007.

[101] Z. Chen, J. Chen, and T. Qiu. Spike extraction of epileptic waves in EEG based on EMD. *Sheng Wu Yi Xue Gong Cheng Xue Za Zhi*. vol. 24, no. 5, pp. 973-977, 2007. (in Chinese).

[102] Y. Zhu, M. Chu, T. Qiu, and H. Bao. An EMD based epileptic spike detection method. *Sheng Wu Yi Xue Gong Cheng Xue Za Zhi*. vol. 25, no. 2, pp. 275-279, 2008. (in Chinese).

[103] J. S. Barlow. EEG transient detection by matched inverse digital filtering. *Electroencephalography and clinical neurophysiology*, vol. 48, no. 2, pp. 246-248, 1980.

[104] P. Guedes de Oliveira, C. Queiroz, and F. Lopes da Silva. Spike detection based on a pattern recognition approach using a microcomputer. *Electroencephalography and clinical neurophysiology*, vol. 56, no. 1, pp. 97-103, 1983.

[105] P. J. Durka. Adaptive time-frequency parametrization of epileptic spikes. *Phys Rev E Stat Nonlin Soft Matter Phys.*, vol. 69, no. 5 Pt 1, 2004

[106] P. Valenti, E. Cazamajou, M. Scarpettini, A. Aizemberg, W. Silva, and S. Kochen. Automatic detection of interictal spikes using data mining models. *Journal of Neuroscience Methods*, vol. 150, no. 1, pp. 105-110, 2006.

[107] K. Polat and S. Gunes. Classification of epileptiform EEG using a hybrid system based on decision tree classifier and fast Fourier transform. *Applied Mathematics and Computation*, vol. 187, no. 2, pp. 1017-1026, 2007.

[108] Z. H. Inan, and M. Kuntalp. A study on fuzzy C-means clustering-based systems in automatic spike detection. *Computers in biology and medicine*, vol. 37, no. 8, pp. 1160-1166, 2007.

[109] E. Ubeyli. Wavelet/mixture of experts network structure for EEG signals classification. *Expert Systems with Applications*, vol. 34, no. 3, pp. 1954-1962, 2008.

[110] A. K. K. Keshri, R. K. Sinha, R. Hatwal, and B. N. Das. Epileptic spike recognition in electroencephalogram using deterministic finite automata. *Journal of medical systems*, vol. 33, no. 3, pp. 173-179, 2009.

[111] F. H. Lopes da Silva, K. van Hulten, J. G. Lommen, W. Storm van Leeuwen, C. W. van Veelen, and W. Vliegenthart. Automatic detection and localization of epileptic foci. *Electroencephalography and clinical neurophysiology*, vol. 43, no. 1, pp. 1-13, 1977.

[112] S. R. Benbadis and W. O. Tatum. Overintepretation of EEGs and misdiagnosis of epilepsy. *Journal of clinical neurophysiology*, vol. 20, no. 1, pp. 42-44, 2003.

[113] S. R. Benbadis. Errors in EEGs and the misdiagnosis of epilepsy: importance, causes, consequences, and proposed remedies. *Epilepsy & behavior: E&B*, vol. 11, no. 3, pp. 257-262, 2007.

[114] S. R. Benbadis and K. Lin. Errors in EEG interpretation and misdiagnosis of epilepsy. Which EEG patterns are overread? *European neurology*, vol. 59, no. 5, pp. 267-271, 2008.

[115] S. R. Benbadis. The differential diagnosis of epilepsy: a critical review. *Epilepsy & behavior: E&B*, vol. 15, no. 1, pp. 15-21, 2009.

[116] S. R. Benbadis. The tragedy of over-read EEGs and wrong diagnoses of epilepsy. *Expert review of neurotherapeutics*, vol. 10, no. 3, pp. 343, 2010.

Chapter 2 A real-time data classification system for accurate analysis of neuro-biological signals

Repeat references:
[11] [15] [16] [17] [18] [19] [20] [21] [22] [23] [13] [14] [12]

[117] Z. R. Chen, W. X. Hong and C. W. Wang, Fuzzy clustering algorithm of kernel for gene expression data analysis, *ICIC Express Letters*, vol.3, no.4 (B), pp. 1435-1440, 2009.

[118] T. Yamaguchi, K. Nagata, P.Q. Truong, M. Fujio, K. Inoue and G. Pfurtscheller, Pattern recognition of EEG signal during motor imagery by using SOM, *Int J*

Innov Comput I., vol. 4, no. 10, pp. 2617-2630, 2008.

[119] Y. J. Chen, K. C. Lin and J. J. Lin, Group sequential analysis of incomplete longitudinal ordinal data, *ICIC Express Letters*, vol. 3, no. 4 (B), pp. 1453-1458, 2009.

[120] M. Nakamura, Q. Chen, T. Sugi, A. Ikeda and H. Shibasaki, Technical quality evaluation of EEG recording based on electroencephalographers' knowledge, *Med Eng Phys.*, vol. 27, no. 1, pp. 93-100, 2005.

Chapter 3 An automatic spike detection system based on elimination of false positives using the large area context in the scalp EEG

Repeat references:

[24] [33] [36] [51] [52] [53] [89] [91] [63] [68] [69] [71] [77] [100] [94] [95] [92] [93] [108] [110] [54] [55] [79] [80] [81] [25] [28] [29] [32] [30] [31] [113] [1] [48]

[121] N. Acir and C. Gzelis, Automatic spike detection in EEG by a two-stage procedure based on support vector machines, *Comput Biol Med.*, vol. 34, no. 7, pp. 561-575, 2004.

[122] T. P. Exarchos, A. T. Tzallas, D. I. Fotiadis, S. Konitsiotis, and S. Giannopoulos, EEG transient event detection and classification using association rules, *IEEE Trans Inf Technol Biomed.*, vol. 10, no. 3, pp. 451-457, 2006.

[123] M. Nakamura, H. Shibasaki, K. Imajoh, S. Nishida, R. Neshige, and A. Ikeda, Automatic EEG interpretation: a new computer-assisted system for the automatic integrative interpretation of awake background EEG, *Electroencephalogr Clin Neurophysiol.*, vol. 82, no. 6, pp. 423-431, 1992.

[124] M. Nakamura, T. Sugi, A. Ikeda, R. Kakigi, and H. Shibasaki, Clinical application of automatic integrative interpretation of awake background EEG: quantitative interpretation, report making, and detection of artifacts and reduced vigilance level, *Electroencephalogr Clin Neurophysiol.*, vol. 98, no. 2, pp. 103-112, 1996.

[125] T. Sugi, M. Nakamura, A. Ikeda, and H. Shibasaki, Automatic integrative interpretation system for awake EEG including spike detection, *Trans. IEE of Japan*, vol. 122-C, no. 9, pp. 1573-1580, 2002. (in Japanese)

Chapter 4 Automatic spike detection based on real-time multi-channel template

Repeat references:

[44] [62] [91]

[126] R. Meier, H. Dittrich, A. Schulze-Bonhage, and A. Aertsen, Detecting epileptic seizures in long-term human EEG: a new approach to automatic online and real-time detection and classification of polymorphic seizure patterns, *J Clin*

Neurophysiol., vol. 25, no. 3, pp. 119-131, 2008.

[127] K. M. Kelly, D. S. Shiau, R. T. Kern, J. H. Chien, M. C. Yang, K. A. Yandora, J. P. Valeriano, J. J. Halford, and J. C. Sackellares, Assessment of a scalp EEG-based automated seizure detection system, *Clin Neurophysiol.*, vol. 121, no. 11, pp. 1832-1843, 2010.

[128] Z. F. Ji, T. Sugi, S. Goto, X. Y. Wang, A. Ikeda, T. Nagamine, H. Shibasaki, and M. Nakamura, Automatic EEG spike detection adaptable to state of background activities, in *The 29th International Congress of Clinical Neurophysiology*, Kobe, October 2010.

[129] Z. F. Ji, T. Sugi, S. Goto, X. Y. Wang, and M. Nakamura, "Multi-channel template extraction for automatic EEG spike detection," in *The 2011 IEEE/ICME International Conference on Complex Medical Engineering*, Harbin, May 2011.

Publications

A. Journal paper

[1] Zhanfeng Ji, Takenao Sugi, Satoru Goto, Xingyu Wang and Masatoshi Nakamura, "A real-time data classification system for accurate analysis of neuro-biological signals", *International Journal of Innovative Computing, Information and Control*, pp. 73-82, Vol.7, No.1, 2011.

[2] Zhanfeng Ji, Takenao Sugi, Satoru Goto, Xingyu Wang, Akio Ikeda, Takashi Nagamine, Hiroshi Shibasaki and Masatoshi Nakamura, "An automatic spike detection system based on elimination of false positives using the large area context in the scalp EEG", *IEEE Transactions on Biomedical Engineering*, pp. 2478-2488, Vol.58, No.9, 2011 .

B. Proceedings of international conferences

[1] Zhanfeng Ji, Takenao Sugi, Satoru Goto, Xingyu Wang and Masatoshi Nakamura, "Data Classification for Analyzing Characteristics of Electrocardiogram and Electroencephalogram under Continuous Long-Time Mental Calculation and Rest", *2nd International Conference on Biomedical Engineering and Informatics*, Tianjin, October 2009.

[2] Zhanfeng Ji, Takenao Sugi, Satoru Goto, Xingyu Wang and Masatoshi Nakamura, "Real-time Data Classification for EEG and ECG Analysis Based on Artifacts Detection, *Proceedings of the 41st ISCIE international symposium on stochastic systems theory and its applications*, Kobe, Nov, 2009.

[3] Zhanfeng Ji, Takenao Sugi, Satoru Goto, Xingyu Wang, Akio Ikeda, Takashi Nagamine, Hiroshi Shibasaki and Masatoshi Nakamura, "Automatic EEG Spike Detection Adaptable to State of Background Activities", *29th International Congress of Clinical Neurophysiology*, Kobe, October 2010.

[4] Zhanfeng Ji, Takenao Sugi, Satoru Goto, Xingyu Wang, Akio Ikeda, Takashi Nagamine, Hiroshi Shibasaki and Masatoshi Nakamura, "Multi-channel Template Extraction for Automatic EEG Spike Detection", *The 2011 IEEE/ICME International Conference on Complex Medical Engineering*, Harbin, May 2011.

[5] Zhanfeng Ji, Xingyu Wang, Takenao Sugi, Satoru Goto and Masatoshi Nakamura, "Automatic spike detection based on real-time multi-channel template", 4*nd*

International Conference on Biomedical Engineering and Informatics, Shanghai, October 2011.

C. Proceedings of domestic conferences

[1] Zhanfeng Ji, Takenao Sugi, Satoru Goto, Xingyu Wang, Akio Ikeda, Takashi Nagamine, Hiroshi Shibasaki and Masatoshi Nakamura, "Multi-channel Detection of EEG Spikes Adaptable to Individual Background Activity", *ME Kyushu*, Kyushu University, Fukuoka, March 2010.

[2] Zhanfeng Ji, Takenao Sugi, Satoru Goto, Xingyu Wang, Akio Ikeda, Takashi Nagamine, Hiroshi Shibasaki and Masatoshi Nakamura, "Topographical analysis for automatic EEG spike detection", *ME Kyushu*, Kyushu University, Fukuoka, January 2011.

Index of publications corresponding to the chapters

Chapters	Journal	Conference
Chapter 2 A real-time data classification system for accurate analysis of neuro-biological signals	A[1]	B[1], B[2]
Chapter 3 An automatic spike detection system based on elimination of false positives using the large area context in the scalp EEG	A[2]	B[3], B[4], C[1], C[2]
Chapter 4 Automatic spike detection based on real-time multi-channel template		B[5]